IPPJ-AM-

ATOMIC DATA FOR HYDROGENS IN COLLISIONS WITH ELECTRONS

—ADDENDA TO IPPJ-AM-46—

H.TAWARA, Y.ITIKAWA, H.NISHIMURA
AND M.YOSHINO

INSTITUTE OF PLASMA PHYSICS
NAGOYA UNIVERSITY

NAGOYA, JAPAN

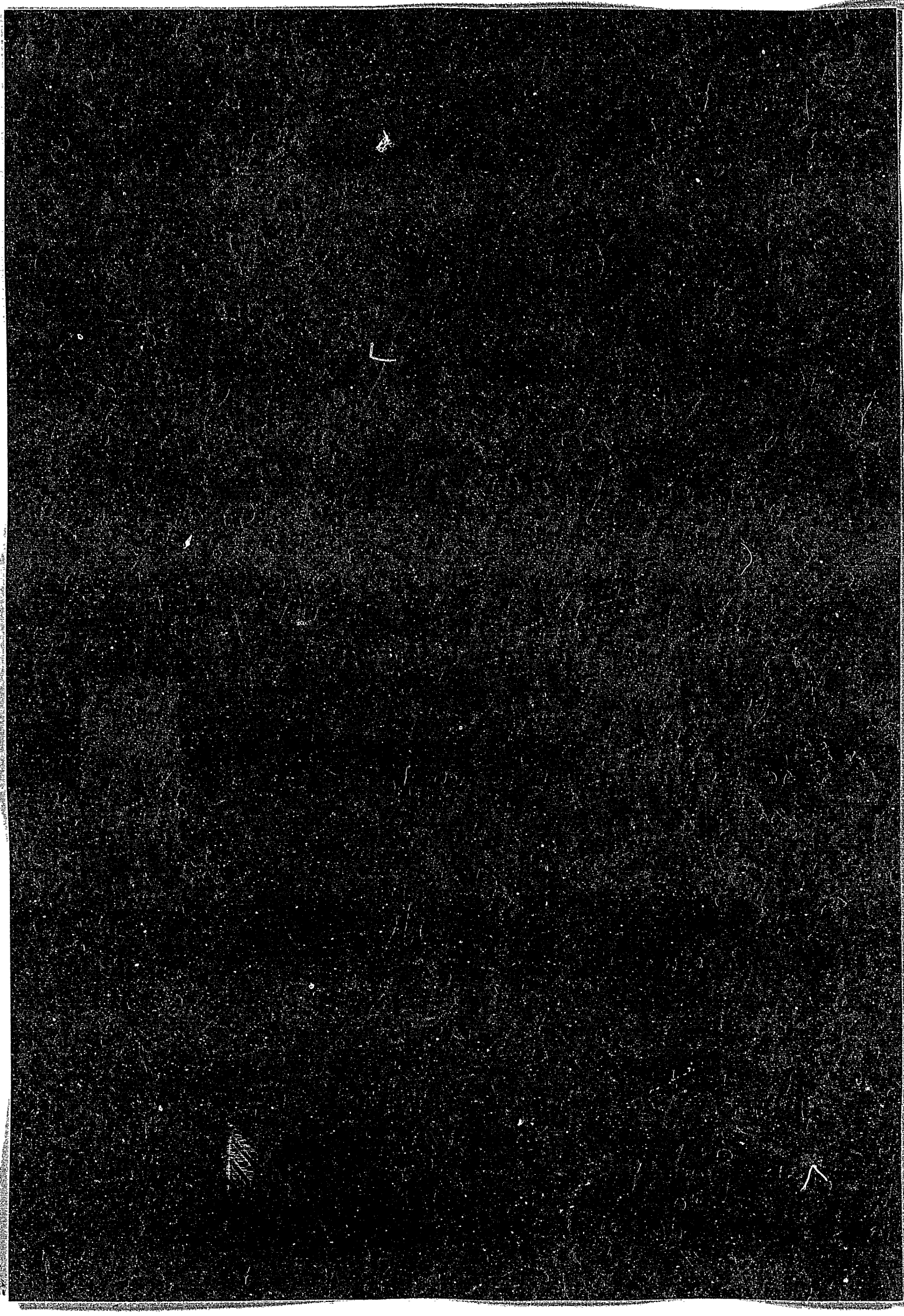

IPPJ-AM-55

ATOMIC DATA FOR HYDROGENS IN COLLISIONS WITH ELECTRONS
– ADDENDA TO IPPJ-AM-46 –

H. Tawara, Y. Itikawa[1], H. Nishimura[2] and M. Yoshino[3]

Institute of Plasma Physics, Nagoya University
Chikusa-ku, Nagoya 464, Japan

October 1987

Present address:
1) Institute for Space and Aeronautical Sciences, Tokyo 153
2) Physics Department, Niigata University, Niigata 950-21
3) Shibaura Institute of Technology, Ohmiya 330

Abstract

This report is addenda to our previous report IPPJ-AM-46 published in September, 1986 which is concerned with atomic data involving hydrogens relevant to the edge plasma studies. The main emphasis of the present report is placed on the survey of characteristics of hydrogen atoms and ions produced through the dissociation or excitation of hydrogen molecules by electron impact.

I. Introduction

A series of atomic processes involving hydrogens, atomic, molecular or ionic, play a significant role in understanding the behavior of edge or boundary plasmas in fusion devices. We have recently compiled atomic data for such processes which seem to be relevant and important for such a investigation[1]. There atomic data for about 150 processes for hydrogens in collisions with electrons, photons and atomic, molecular hydrogens and their ions are given in figures or tables. In understanding and modelling hydrogen plasmas, the behavior of their constituents such as atoms, molecules, or ions has to be known. For that, the potential energy diagram of molecules is most convenient (see Fig.1). In Fig.2 are shown summaries of total cross sections for various excitation processes of molecules with the reference of ionization cross sections for molecular hydrogens by electron impact which have been well investigated[1]. It is clear that, at low energies 10^{-1}-a few eV, the rotational excitation and then vibrational excitation of molecules are dominant and above a few eV the electronic excitation processes play a role. Most of these electronic excitations result in dissociation of molecules where atomic hydrogens or hydrogen ions(protons) are produced. The energy distribution and angular distribution of hydrogen atoms from these dissociative excitation/ionization processes are known to be important and to play a key role in modelling the boundary plasmas which are discussed in section II.

These excitation processe are closely related to the line emissions from hydrogen atoms in the excited states. In Fig.3 are shown summaries of the cross sections for emissions of Lyman and Balmer lines as well as Lyman and Werner bands.[1] These emission data are necessary for estimating the cooling of plasmas through photon emissions. Here it is noted that Lyman band data include the contribution of cascades from the upper excited states, meanwhile their contribution to Werner band is minimal.

In section III are discussed similar data on protons resulting from dissociative ionizations. The cross sections

for production of total protons and H_2^+ ions from H_2 molecules are shown in Fig. 4, together with those for ionization of the ground state and metastable 2s atoms. In Fig. 5 are shown the cross sections for various processes including the dissociative recombination, dissociation and proton production from H_2^+ ions under electron impact. At low energies, the dissociative recombination is dominant over other processes, where at intermediate to high energies dissociation and ionization become dominant. Similar data for H_3^+ ions are shown in Fig.6.

It should be noted that the rotational/vibrationl excitation processes as well as electronic excitation processes are significantly influenced by the densities of plasmas as discussed by Janev et al.[2] which effect is not included here.

References

1) H. Tawara, Y. Itikawa, Y. Itoh, T. Kato, H. Nishimura, S. Ohtani, H. Takagi, K. Takayanagi, and M. Yoshino, IPPJ-AM-46 (Institute of Plasma Physics, Nagoya University, 1986)

2) R.K. Janev, D.E. Post, W.D. Langer, K. Evans, D.R. Heifetz and J. C. Weisheit, PPPL-2045 (Princeton Plasma Physics Laboratory, 1983)

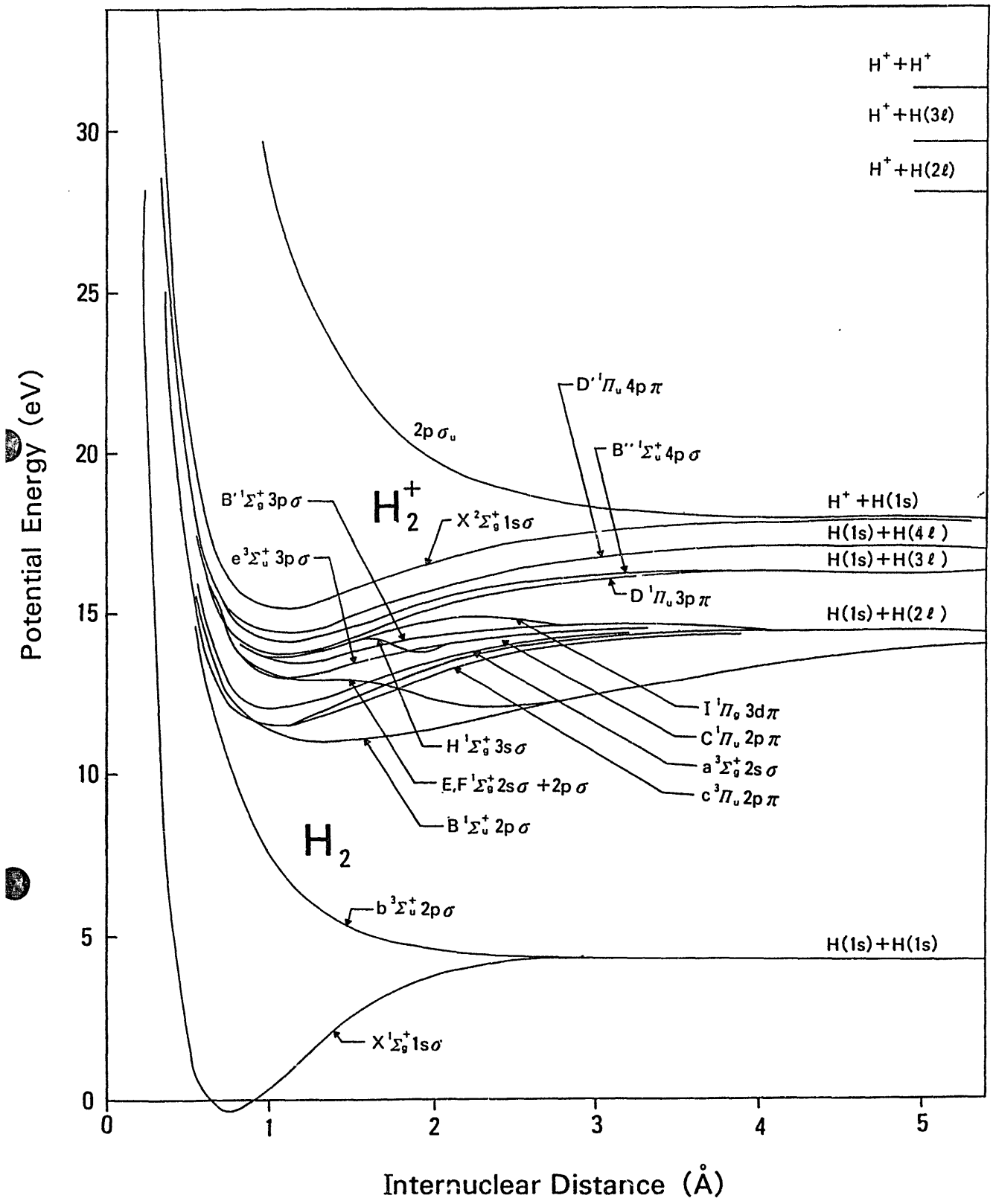

Fig. 1 The potential energy diagram of H_2 and H_2^+.

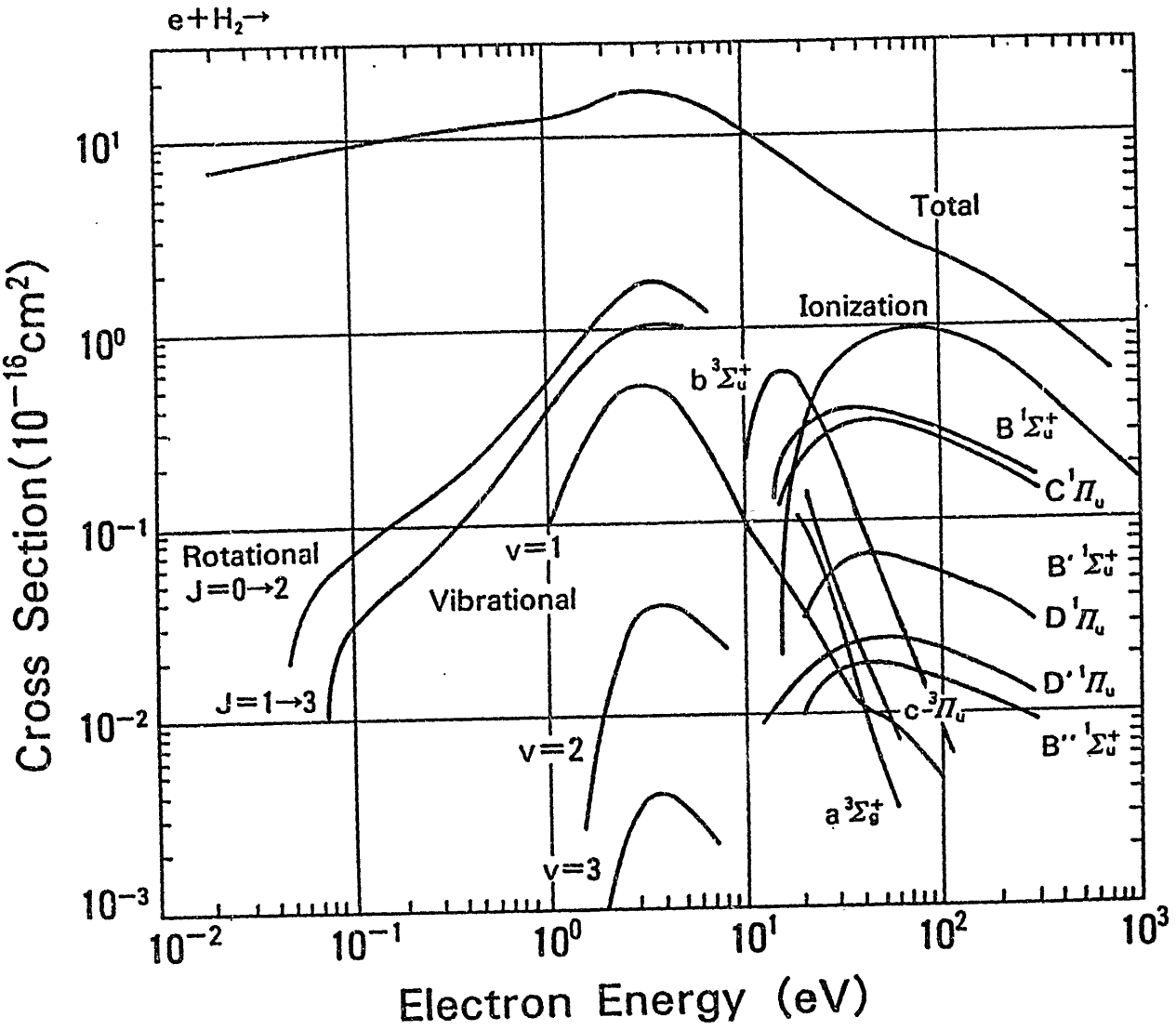

Fig. 2 The cross sections for various excitation processes of H_2 molecules by electron impact. Note that recent data by Nishimura and Danjo[1] and Khakoo et al.[2] are included.

1) H.Nishimura and A.Danjo, J.Phys. Soc. Japan 55 (1986) 3031:

2) M.A. Khakoo, S.Trajmar, R. McAdams and T.W. Shyn, Phys. Rev. A 35 (1987) 2832

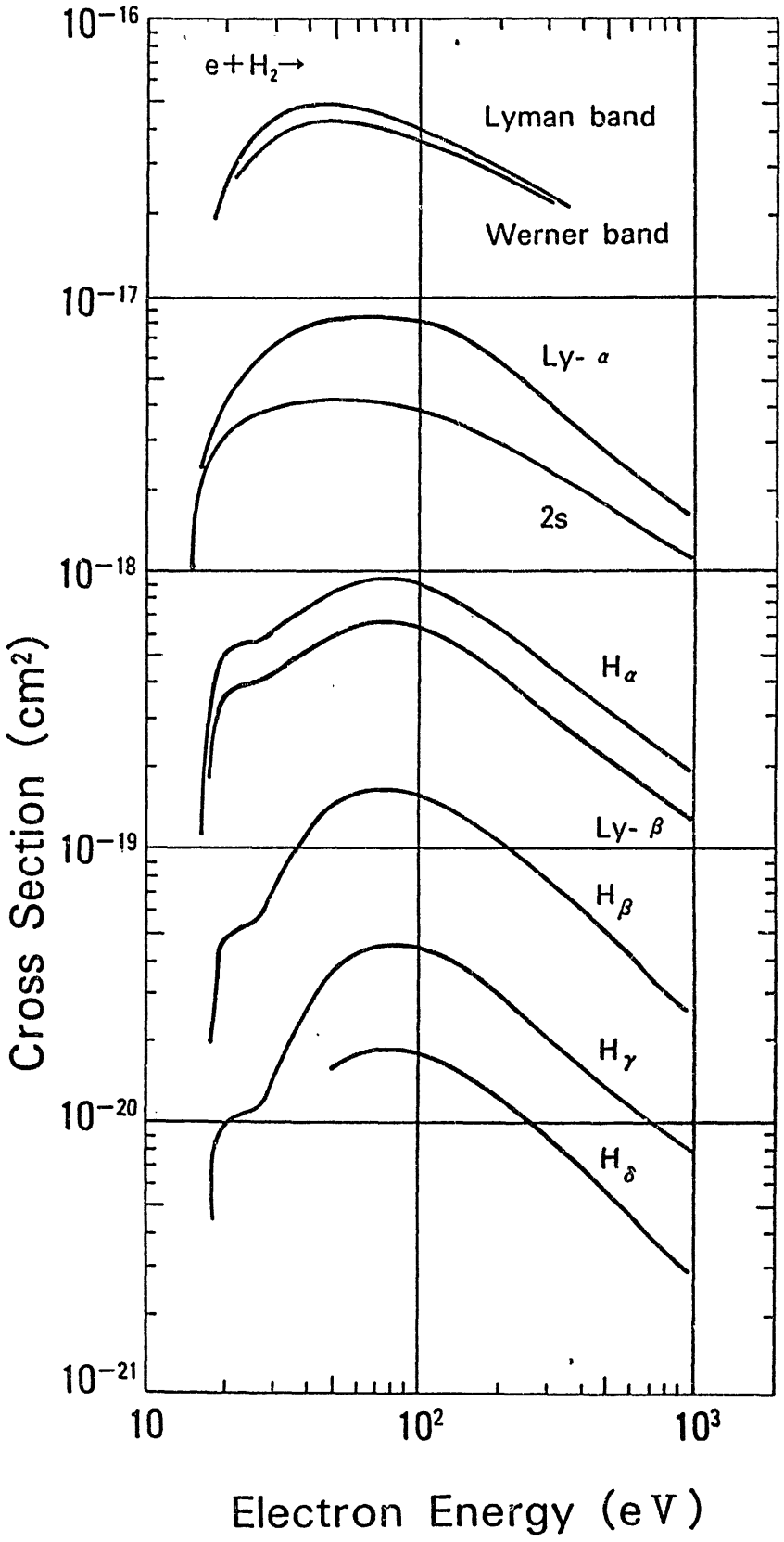

Fig. 3 The cross sections for various line emissions from H_2 molecules by electron impact (See a note on the next page).

Note : The cross sections shown in the preceding page are based upon the normalizing cross sections at 100 eV by Shemansky et al.[1] More recent data became available as follows (at 100 eV in units of $10^{-18}cm^2$) :

Shemansky et al.[1]	8.12 ± 1.20
Van Zyl et al.[2]	7.22 ± 1.36
Woolsey et al.[3]	7.13 ± 0.59
McPherson et al.[4]	6.57 ± 0.53

References

1) D.E. Shemansky, J.M. Ajello and D.T. Hall, Astrophys. J. 296 (1985) 765

2) B.Van Zyl, M.W.Gealy and H.Neumann, Phys. Rev. A 31 (1985) 2922

3) J.M. Woolsey, J.L. Forand and J.W.McConkey, J.Phys. B 19 (1986) L493

4) A. McPherson, N.Rouze, W.B. Westveld and J.S.Risley, Appl. Opt. 25 (1986) 298

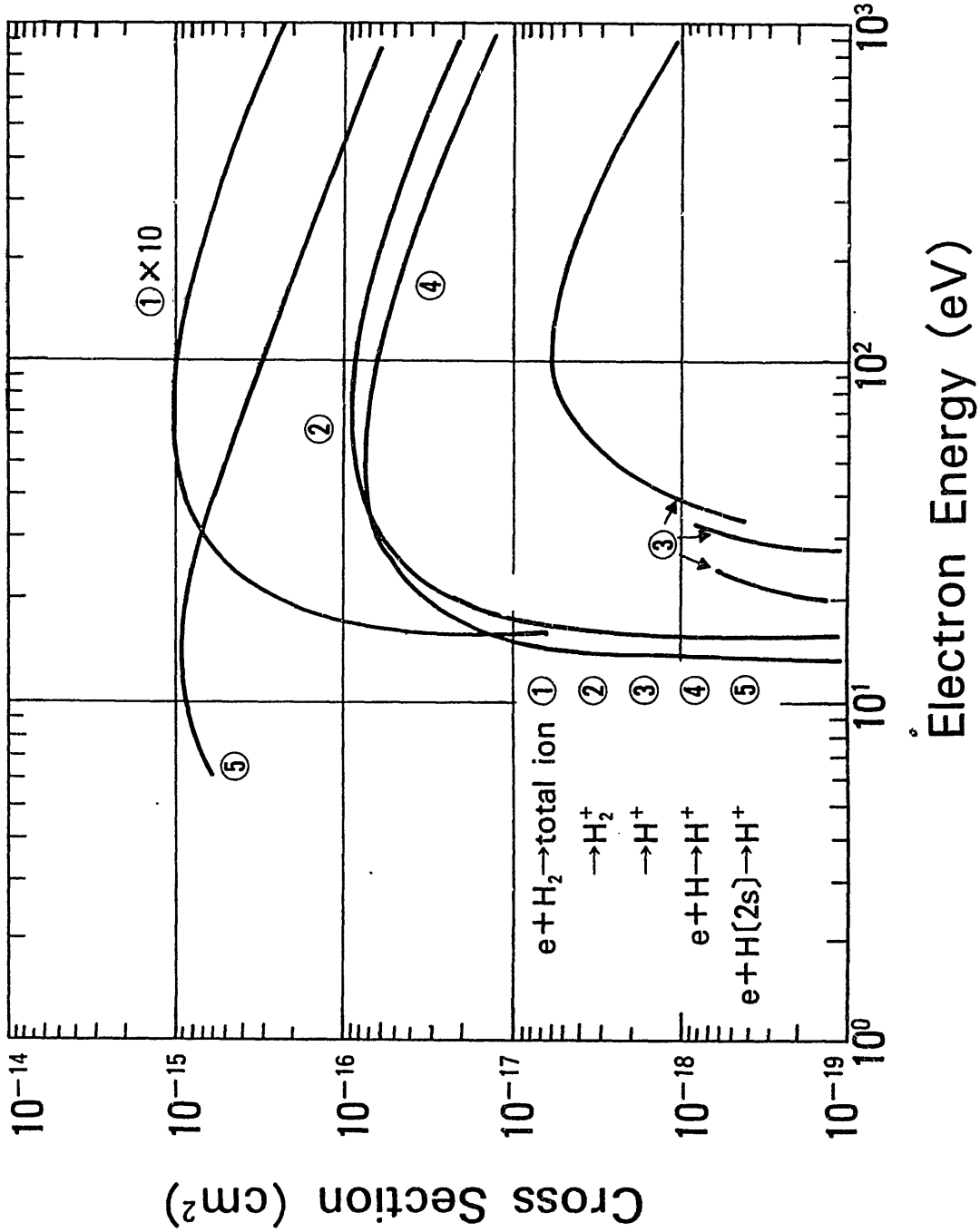

Fig. 4 Cross sections for production of ions from H_2 molecular targets by electron impact, together with those from atomic hydrogens and metastable hydrogens.

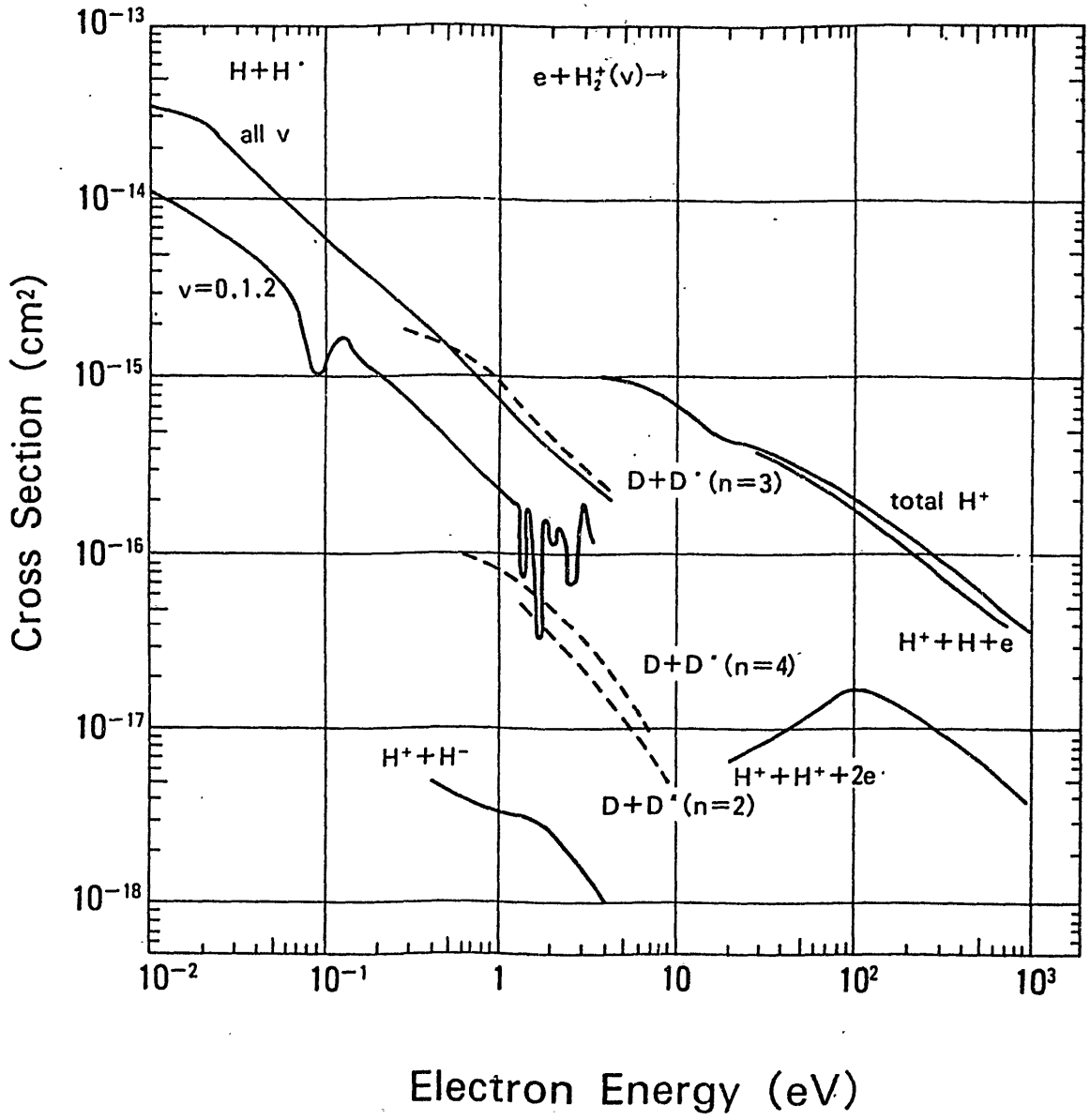

Fig. 5 The cross sections for various processes of H_2^+ ions by electron impact.

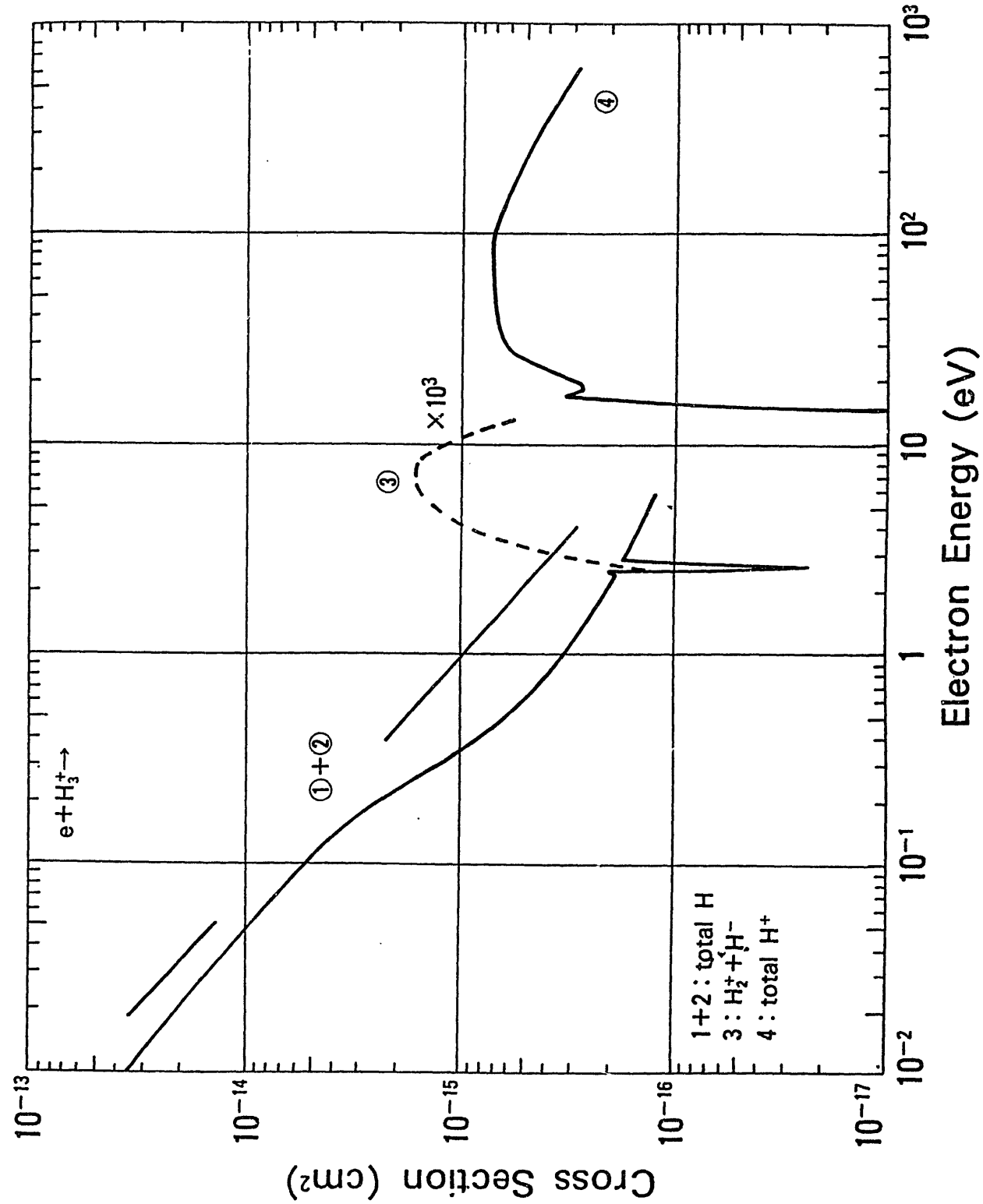

Fig. 6 The cross sections for various processes of H_3^+ ions by electron impact.

II. Hydrogen atoms from dissociative excitation/ionization of molecular hydrogens.

Various data involving production of atomic hydrogens, either in the ground state or in the excited states, have been obtained. The characteristics of the atomic hydrogens can be understood qualitatively through the potential energy diagram. Because of difficulties in detecting them, in particular atoms in the ground state, only a few systematic investigations have been carried out until now.

1. The ground state atoms

Total cross sections for production of two atoms both in the ground state, H(1s), through the process

$$e + H_2 \rightarrow H_2(b^3\Sigma_u^+) \rightarrow H(1s) + H(1s) \qquad (II\text{-}1)$$

are known[1]. However, their energy distributions and angular distributions are not yet investigated . The average kinetic energy of both atoms is estimated to be around 2-3 eV each from the energy loss spectrum and from the energy diagram and hydrogen atoms themselves are expected to be isotropically distributed. In order to investigate the behaviour of H(1s), powerful lasers are necessary to excite both of them simultaneously. This is one of the important and basic problems in understanding dissociation of molecular hydrogens.

With increasing the impact energy, hydrogen atoms in the ground state, H(1s), origintate not only from the lowest repulsive $b^3\Sigma_u^+$ state mentioned above but also from a number of (singly) excited states (see Fig. 1). From the latter excited states, usually two groups of H(1s) with different energies are produced: one is the near-zero energy atom (for exapmle, from the attractive $^2\Sigma_g^+$ $1s\sigma$ state resulting in dissociation into $H^+ + H(1s)$) and the other one relatively high energy atom (from the corresponding repulsive $2p\sigma_u$ $^2\Sigma_u^+$ state). In between there are a series of the channels contributing to production of these atoms resulting in H(1s) + $H^*(n,\ell)$. By looking at the potential energy diagram, the

energy distribution of H(1s) atoms is estimated as shown on the left hand side of Fig.1. Unfortunately little is known on the behavior of H(1s) atoms produced through dissociation of H_2 molecules.

Very recently a technique has been developed for measuring the energy distribution of the dissociated ground state hydrogen atoms, based upon the deflection of these atoms in non-uniform magnetic field due to their magnetic moment.

2. Atoms in the excited states

If the product hydrogen atoms are in the excited states, $H(n,\ell)$, they decay into lower states, resulting in the emission of photons. By looking at these photons, more precisely by observing the Doppler profiles of the photons from these atoms, the velocity and kinetic energy distributions of the product atoms can be known[3] (see Fig.2). The energy distribution of the metastable H(2s) atoms from the process

$$e + H_2 \rightarrow H_2^{**} \rightarrow H^*(2s) + H^*(n,\ell) \qquad \text{(II-2)}$$

was investigated by Leventhal et al.[4] who showed a single slow component with the average energy of 0.21 ± 0.02 eV and two fast components with the energy of 2.3 ± 0.5 and 4.4 + 0.9 eV at the impact energy of 60 eV which were observed at 13° with respect to the electron beam direction. Their results show that the slow component does not change with the observing angle, whereas the fast components do change significantly with the angle. Thus in contrast to the above, for example, at 90° only a single peak corresponding to the energy of 4.7 ± 0.7 eV has been observed. More detailed analysis was made by Spezeski et al.[5] The slow component originates from the attractive singly excited states such as $B^1\Sigma_u^+$, $B'^1\Sigma_u^+$, $e^3\Sigma_u^+$, $E^1\Sigma_g^+$ and $a^3\Sigma_g^+$. On the other hand, the fast components are found to originate from doubly excited, repulsive states. It is inferred from their results that at least two repulsive states with different sysmmetries such as $(2p\sigma)\ (2s\sigma)^{1,3}\Sigma_u^+$ states contribute to the fast components.

No quantitative studies on the energy distribution and angular distribution of these components have been reported. The following particular process

$$e + H_2 \rightarrow H^+ + H^*(2s) \qquad \text{(II-3)}$$

has been investigated by the coincidence technique between proton and quenched Lyman - α radiation.[6] The kinetic energy of H(2s) atoms is estimated to be about 4 - 8 eV with a maximum at 5.8 eV, in agreement with the work of Leventhal et al.[4] and concluded that these H(2s) atoms originate mostly from $2s\sigma_g$ with a slight contribution of $3p\sigma_u$ state. Based on their results they tried to determine the potential energy curves for these states. However, no cross section was given.

The state-selective dissociation process

$$e + D_2 \rightarrow D^*(2p) + D^*(2p) \qquad \text{(II-4)}$$

has been studied by the coincidence between two Lyman - α radiations. These atoms in the 2p state originate from the doubly excited states through dissociation. The cross sections for the above process is estimated to be 6×10^{-20} cm^2 with uncertainty of a factor of two at 200 eV impact energy.[7] This small cross section can be understood from the fact that there are other competing exit channels, such as autoionization and highly (singly) excited Rydberg states. Hydrogen atoms in the n=3 states produced through the process

$$e + H_2 \rightarrow H_2^{**} \rightarrow H^*(n=3) + H^*(n,\ell) \qquad \text{(II-5)}$$

are found, by observing the Balmer-α lines, to have two components in their energy distributions[8]: one is the near-zero energy (with the average energy of 0.2 eV) produced through predissociation of vibrational excited states such as $1s\sigma_g$ state or Rydberg states directly dissociated and the other one relatively high energy of 7 eV produced through the repulsive doubly excited states such as $2p\sigma_u$. It is

interesting to note that these Balmer lines originate mainly from 3s and 3d states.[9] However, no quantitative measurements of this process have been reported.
By observing the Balmer-β lines, similar investigations on the production of H(n=4) atoms through the process

$$e + H_2 \rightarrow H_2^{**} \rightarrow H^*(n=4) + H^*(n.\ell) \qquad \text{(II-6)}$$

can be made and it is found that there are three components at zero, 4 and 8 eV, whose threshold energies are 17.1, 24 and 27 eV, respectively.[10] Their production mechanisms are very similar to those for H(n=3) atoms.
The situations are similar in production of H(n=5) atoms through the process

$$e + H_2 \rightarrow H_2^{**} \rightarrow H^*(n=5) + H^*(n,\ell) \qquad \text{(II-7)}$$

where three components are observed: zero, 4 and 7-8 eV, with the threshold energies of 17.5, 26 and 26 eV. At lower energies, a peak for high energy component is located around 4 eV and with increasing the impact energy the peak shifts to 8 eV[11]. This fact suggests that many channels contribute to production of atoms. In principle the angular distributions of their intensities and of their energy can be inferred from measurements of Doppler profiles of the photons as a function of the observing angles. However, no such experiments have been carried out. In fact, the Doppler profiles are found to be dependent not only on the kinetic energy and angular distribution of these atoms but also on the polarization of the photons[12].

References

1) H.Nishimura and A.Danjo, J.Phys. Soc. Japan 55 (1986) 3031: M.A.Khakoo, S.Trajmar, R.McAdams and T.W.Shyn, Phys. Rev. A 35 (1987) 2832.
2) B. Jaduszliwer, Abstract Book of XV ICPEAC(1987, Brighton) p.812

3) R.S.Freund, J.A.Schiavone and P.F.Brader, J.Chem. Phys. 64 (1976) 1122.
4) M.Leventhal, R.T.Robiscoe and K.R.Lea, Phys. Rev. 158 (1967) 49.
5) I.J.Spezeski, O.F.Kalman and L.C.McIntyre, Jr., Phys. Rev. A 22 (1980)1906.
6) H.Cho, K.C.Hsieh and L.C.McIntyre, Jr., Phys. Rev. A 33 (1986) 2290.
7) N.Böse, J.Phys. B 11 (1978) L309.
8) K.Ito, N.Oda, Y.Hatano and T.Tsuboi,Chem. Phys. 17 (1976) 35 :21 (1977) 203.
9) L.D.Weaver and R.H.Hughes, J.Chem. Phys. 52 (1970) 2299.
10) T.Ogawa and M.Higo, Chem. Phys. 52 (1980) 55.
11) M.Higo, S.Kamata and T.Ogawa, Chem. Phys. 66 (1982) 243.
12) N.Takahashi, S.Arai, N.Kouchi, N.Oda and Y.Hatano, J.Phys. B 16 (1983) 1547.

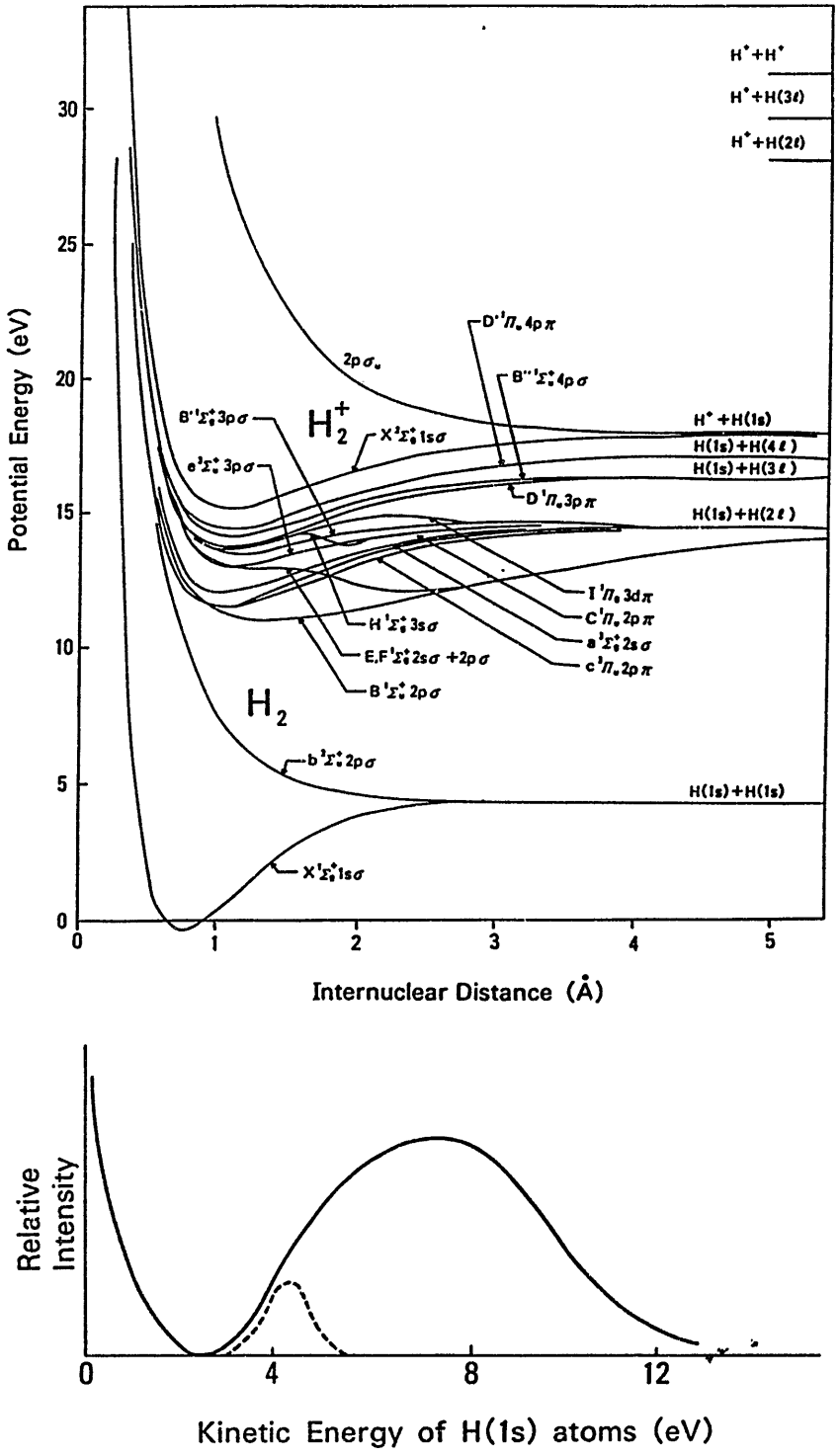

Fig. 1 The potential energy curves of H_2 molecules and the expected energy distribution of H(1s) atoms produced through dissociation. The dotted line corresponds to atomic hydrogens from $b^3\Sigma_u^+$ $2p\sigma$ state at low excitation energies, whereas the solid line does to those from $x^2\Sigma_g^+$ $1s\sigma$ state (near zero energies) and those from $2p\sigma_u$ repulsive state (high energy part).

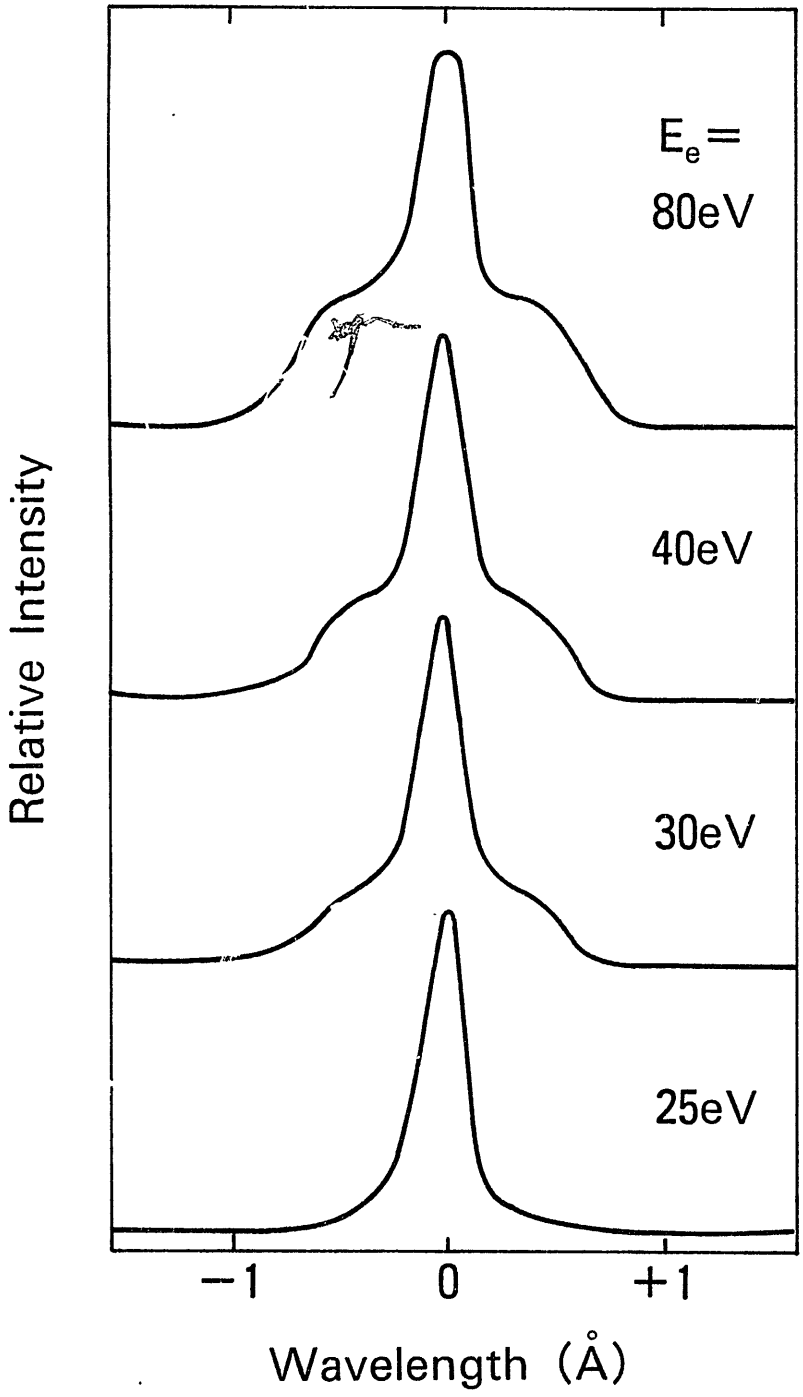

Fig. 2 The Doppler shifted spectral line shapes of H_β line as a function of the electron impact energy.

III. Protons from dissociative ionization of H_2 molecules by electron impact

Proton production from dissociation of H_2 can be understood from Fig.1 where some important potential energy diagrams of H_2, H_2^+ and H_2^{2+} are shown[1]. Looking into Fig.1, the expected energy distribution of protons from the process

$$e + H_2 \rightarrow H^+ + H^*(n,\ell) \qquad \text{(III-I)}$$

can be inferred as shown on the left side of Fig. 1. There are two main components: the first is protons which originate from the transition to $^2\Sigma^+_g$ of H^+_2 and have peak intensity at near-zero energy and the other protons which originate from the repulsive $^2\Sigma^+_g$ state of H^+_2 ions and from other repulsive states of the excited H_2^{+*} ions and therefore have broad energy distribution peaked at the energy of 8 eV, suggesting more contribution from a number of other channels.

Before going into the detailed discussion of the energy distributions and angular distributions, it is important to know contribution of protons to total ions from H_2 molecules by electron impact[2]. At the impact energy lower than the threshold of transition to $^2\Sigma^+_u$ state, protons mainly come from $^2\Sigma^+_g$ state. Crowe and McConkey[3] determined the ratios of protons to H^+_2 ions which increase roughly linearly with the impact energy up to 0.015 at 25 eV from zero at the threshold of 18 eV, approaching the ratios in photon impact (see Fig 2).

The angular distributions of these zero-energy protons are essentially isotropic up to the impact energy of 25 eV, with a forward-backward asymmetry due to the momentum transfer(± 20% at 22.3 eV with respect to that at 90°, see Fig. 3), agreeing with the Dunn prediction for Σ^+_g-Σ^+_g transitions[4]. As the energy of these protons from $^2\Sigma^+_g$ state is of the order of rotational energy of H_2 molecules (0.02 eV), the observed angular distributions of these zero-energy protons could be smeared out and become isotropic, even if initially anisotropic. As their energy is also comparable to the

thermal energy of H_2 molecules, again the initial, if any, anisotropy tends to be smeared out.

Then, Rapp et al.[5] determined the fractions of protons having the energy higher than 2.5 eV by applying the retarding potential and found that these high energy protons ($E_p > 2.5$ eV) consist of roughly 7% (maximum) of total dissociated protons at the impact energy of 120 eV, decreasing with increasing the impact energy (see Fig.4). Note that total protons consist of roughly 10% of total ions. The energy distributions of high energy protons from H_2 molecules were measured by Crowe and McConkey[6] who revealed a number of peaks: those at the energy of 1,2,4 and 8 eV (see Fig.5). The spectrum, where all the peaks seem to have some shoulders, suggests more channels might contribute to the production of protons. These peaks can be explained to be due to a series of the channels located between $^2\Sigma^+_g$ and $^2\Sigma^+_u$ states (see Fig.6). The intensities of these peaks change fairly significantly with the impact energy (see Fig.7). At the energy higher than 50 eV, the peaks at 8 eV become dominant, though the detailed distribution of the proton energy depends on the observing angles. It should be, however, noted that these structures in the energy spectrum observed by Crowe and McConkey were not confirmed by Kallmann[7].

As mentioned above, the angular distributions of protons are dependent on the impact energy and also on the proton energy. Generally speaking, at low impact energies the distribution shows the forward-backward enhancement with a minimum at 90° and at the energy around 100 eV becomes nearly isotropic and at further high energies, say above 300 eV, the intensities become maximum at 90° with forward-backward reduction, though this asymmetry is not so significant as that at low energies. Some examples are shown in Fig.8 where the angular distributions of protons with the energy of 8 eV are given for different impact energies over 50 - 1500 eV[1]. These observed distributions can be understood well by the Born calculations by Zare[8]. According to his theory, the anisotropy is found to be large for high energy protons and

confirmed experimentally (see Fig.9)[7]. This is supported by van Brunt[9] who observed the variation of the angular distribution in proton energy at different angles, suggesting that the peak at 8 eV should have stronger anisotropy, compared with those of lower energy protons. Similar observations were also reported by Crowe and McConkey[6] whose spectra indicate that peaks with lower energies (2 and 4 eV) are relatively isotropic.

References

1) G.H. Dunn and L.J. Kieffer, Phys. Rev. 132 (1963) 2109.
2) H. Tawara and T. Kato, At. Data and Nucl. Data Tables 36 (1987) 167.
3) A. Crowe and J.W. McConkey, J.Phys. B 6 (1973) 2088.
4) G.H. Dunn, Phys. Rev. Letters 8 (1962) 62.
5) P. Rapp, P. Englander-Golden and P.P.Briglia, J. Chem. Phys. 42 (1965) 4081.
6) A. Crowe and J.W.McConkey, Phys. Rev. Letters 31 (1973) 192: J.A. Stockdale, V.E. Anderson, A.E. Carter and L. Deleanu, J.Chem. Phys. 63 (1975) 3886.
7) K.Kallmann, J.Phys. B 11 (1978) 339.
8) R.N. Zare, J.Chem. Phys. 47 (1967) 204.
9) R.J. van Brunt, Phys. Rev. A 16 (1977) 1309: R.J. van Brunt and L.J. Kieffer, Phys. Rev. A 2 (1970) 1293.

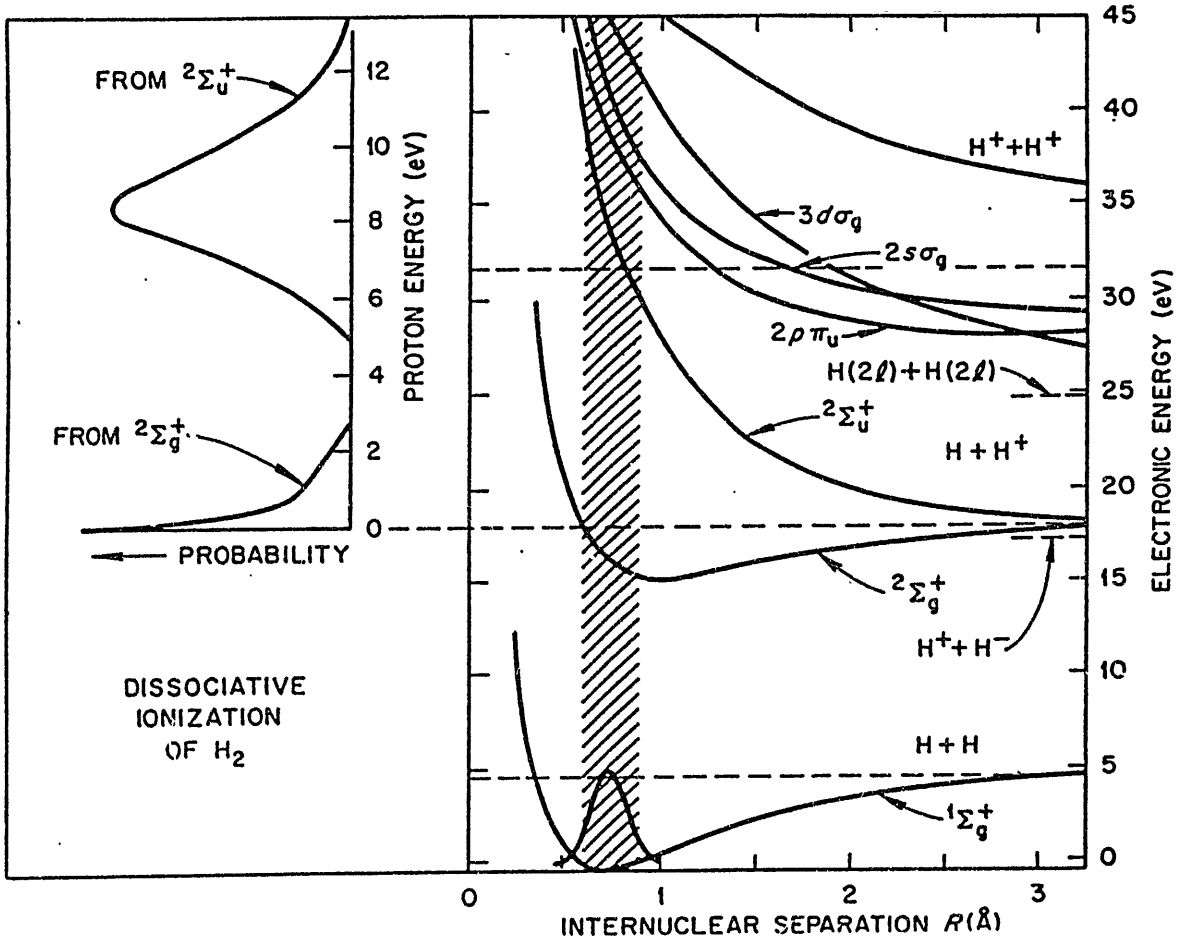

Fig. 1 Potential energy curves of H_2 and H_2^+ and the expected energy distributions of protons produced via $^2\Sigma_g^+$ and $^2\Sigma_u^+$ states of H_2^+ in dissociative ionization of H_2.

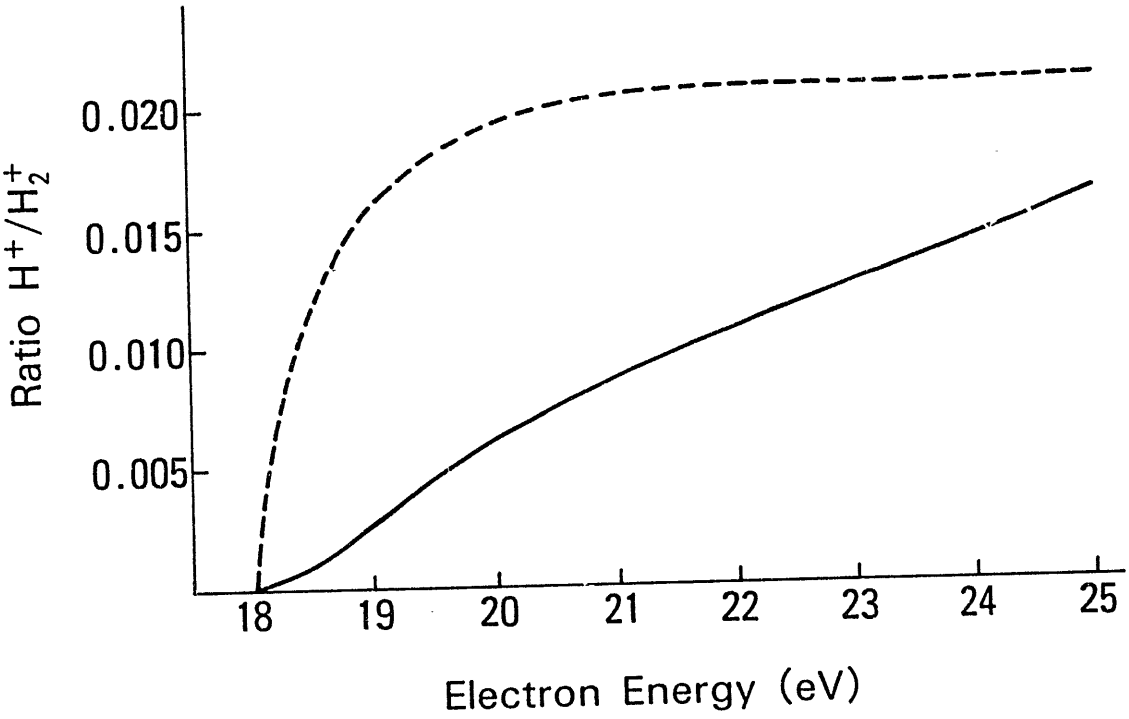

Fig.2 Ratios of H^+/H_2^+ in electron impact. The solid curve shows these ratios in electron impact, whereas the dashed curve represnts those in photon impact.

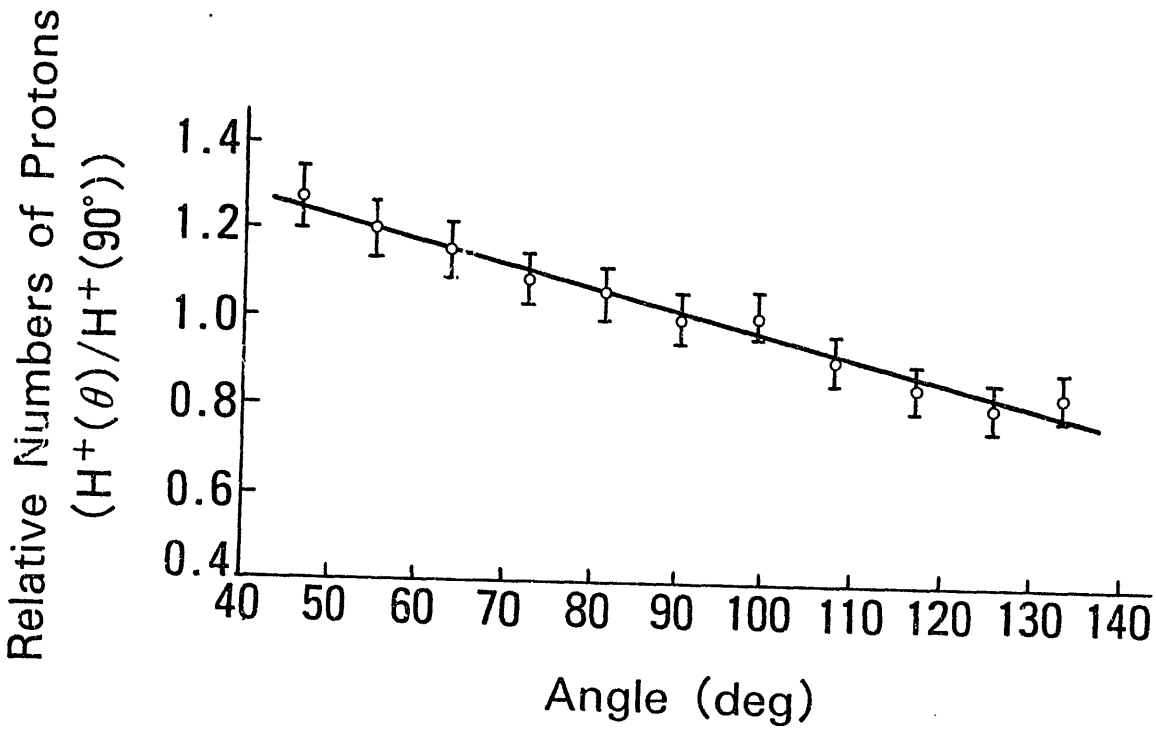

Fig.3 The angular distributions of protons with near-zero energy produced from $^{2}\Sigma_{g}^{+}$ state of H_2^+ ions at the incident energy of 22.3 eV.

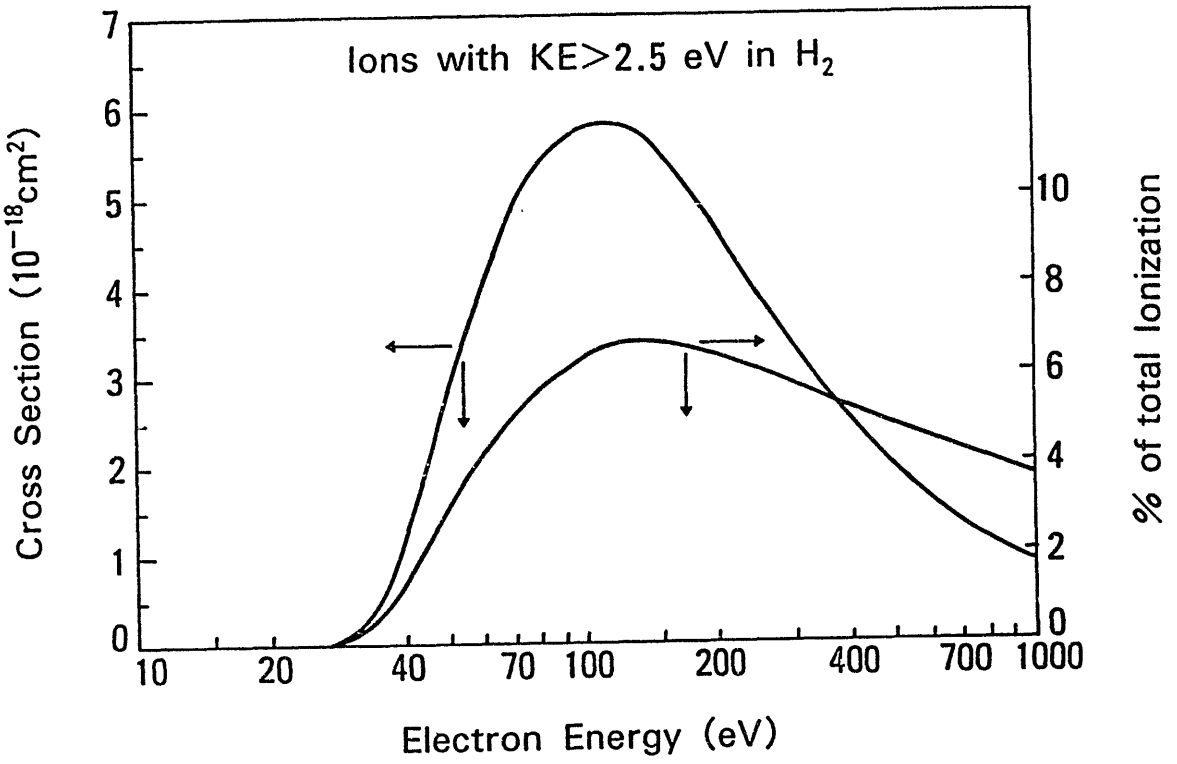

Fig.4 Cross sections of proton production and their fractions with the energy of 2.5 eV.

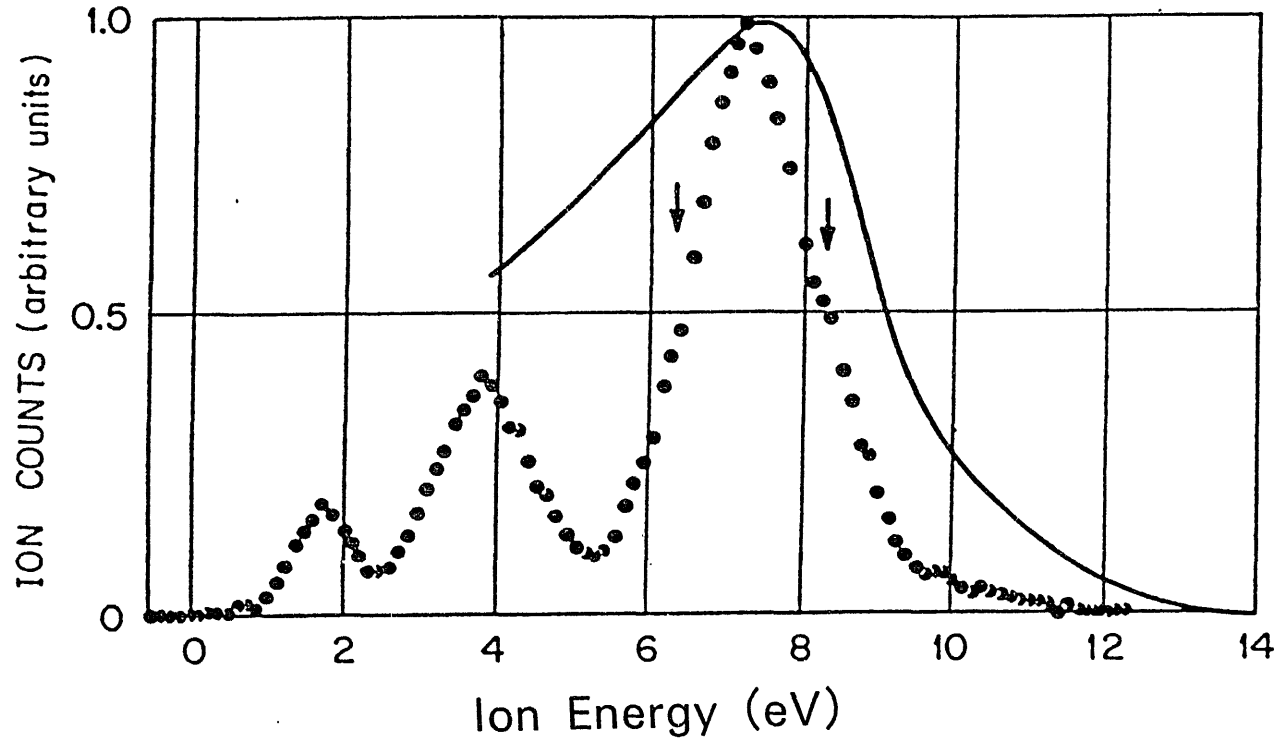

Fig.5 Energy distribution of protons from H_2 in electron impact. Note that protons with near-zero energy from $^2\Sigma_g^+$ state are excluded.

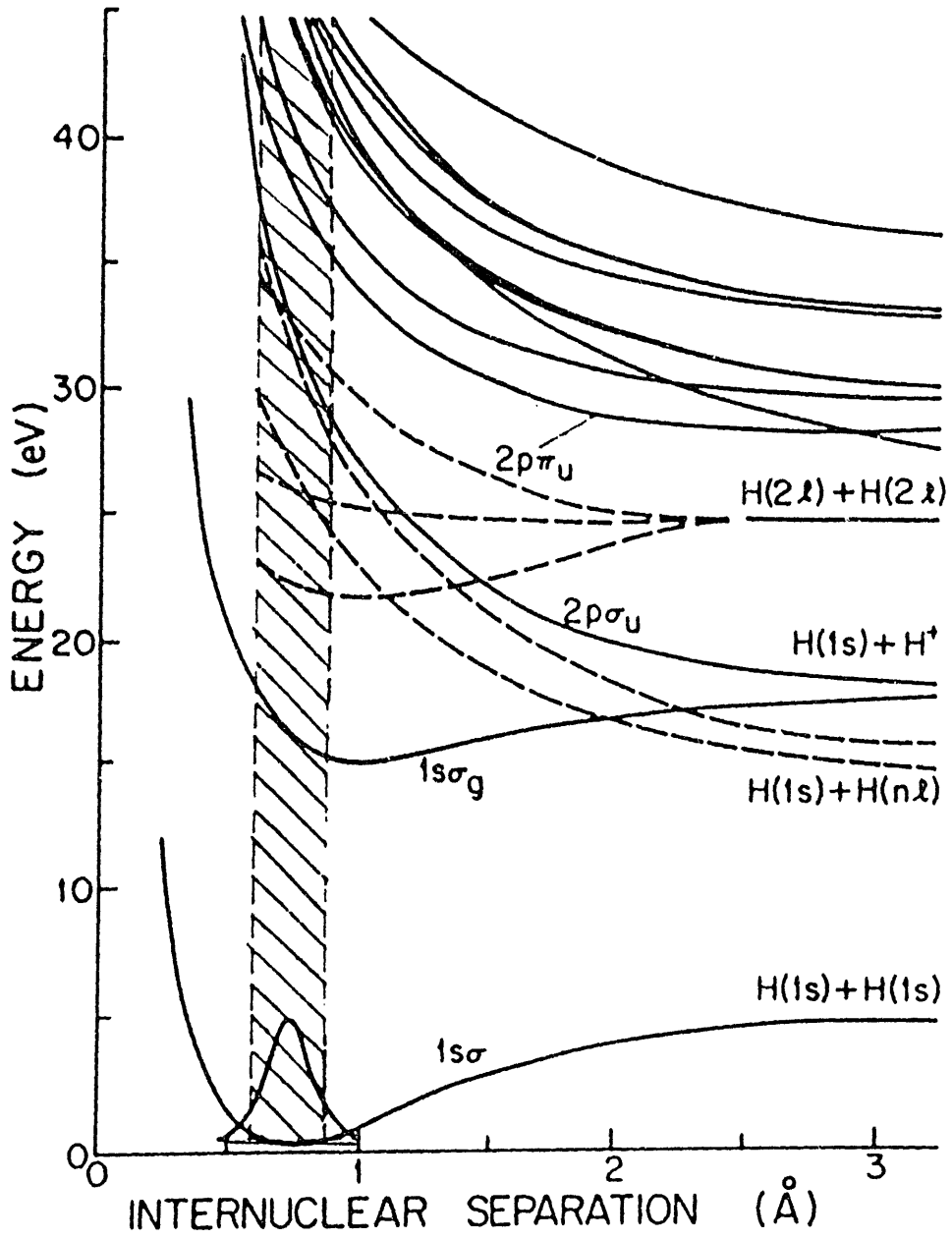

Fig.6 Potential energy diagram including predissociation channels. The dashed curves represent the energy curves of excited states of H_2^* or H_2^{**} which result in production of protons via the predissociation channels.

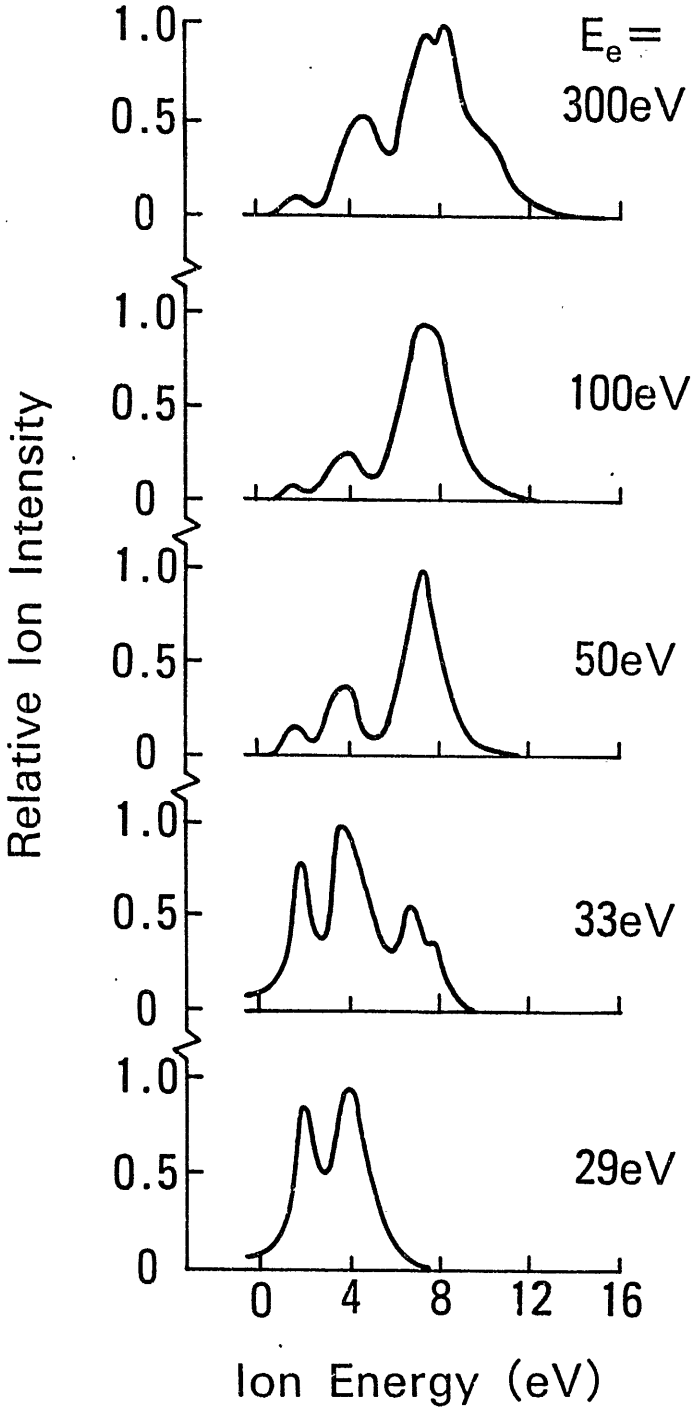

Fig.7 Proton energy spectra at different impact energies. Note that the spectral shapes change with the electron impact energy.

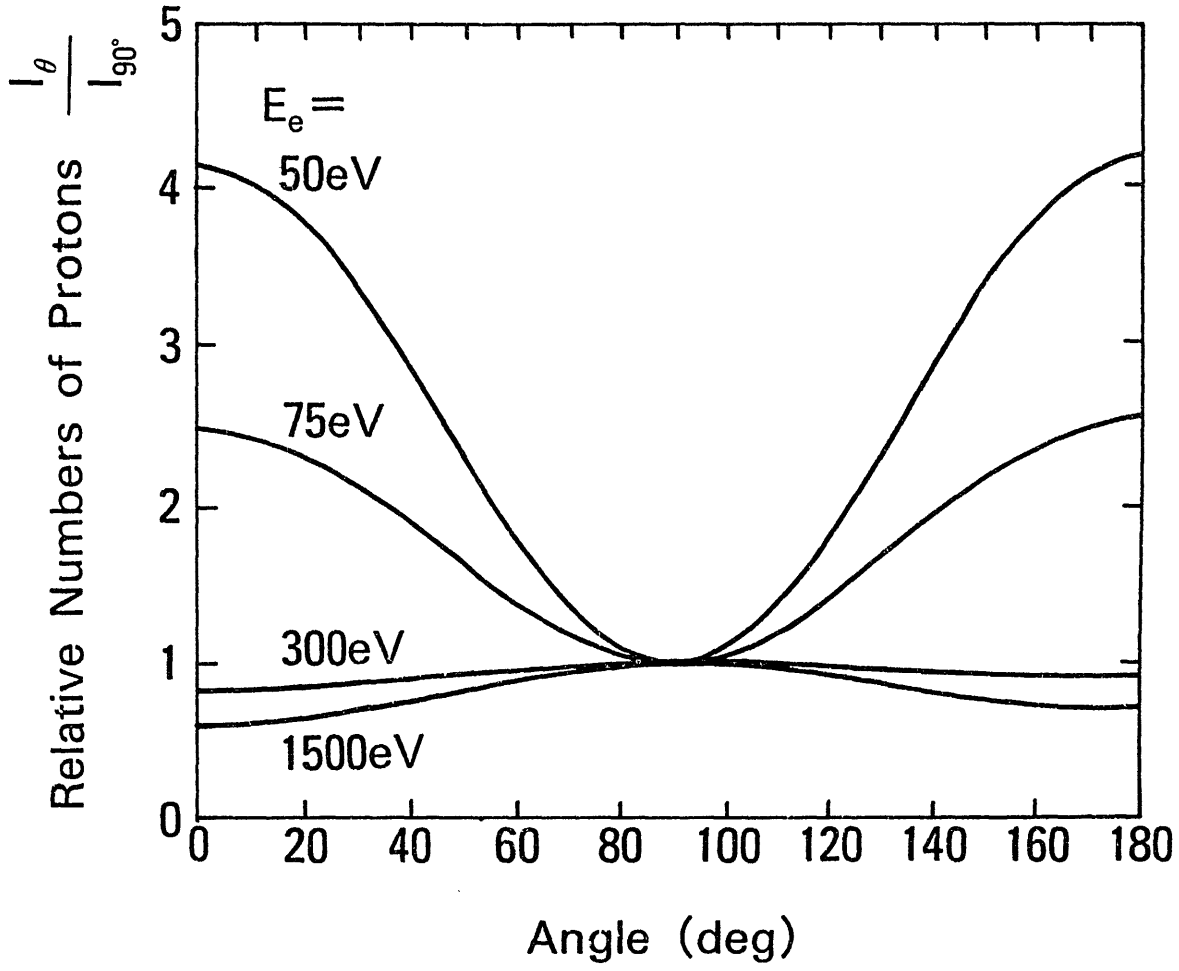

Fig.8 Angular distributions of 8.6 eV protons produced from H_2 targets in various electron impact energies.

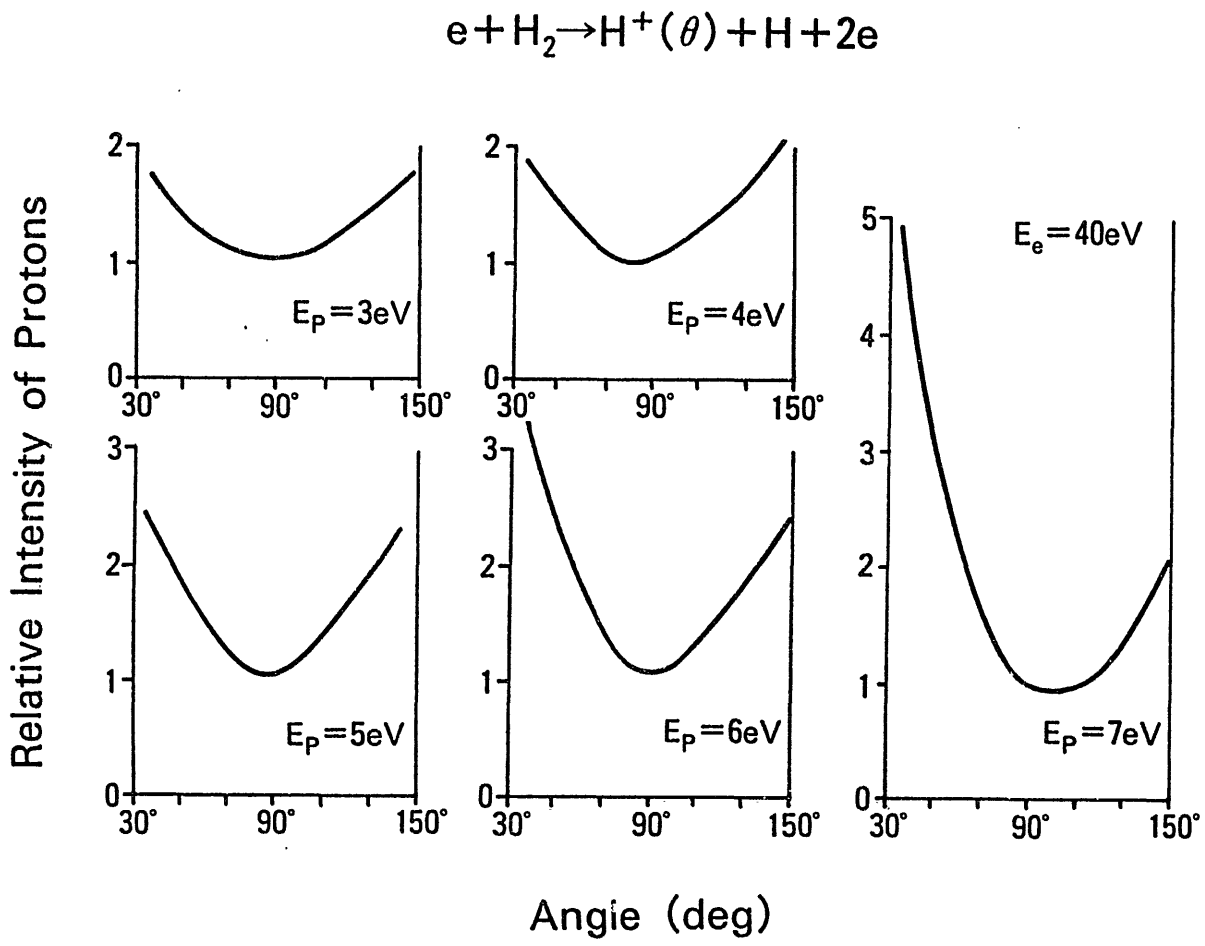

Fig.9 The observed angular anisotropy of protons with different energy at the electron impact energy of 40 eV.

IV. Double ionization of H_2 resulting in production of H_2^{2+} ions

The doubly charged H_2^{2+} molecular ions are dissociated through the repulsive $2p\sigma$ state:

$$e + H_2 \rightarrow H_2^{2+} \rightarrow H^+ + H^+. \qquad (IV-1)$$

Then, the resultant two protons are emitted with high initial kinetic energy. The coincidence measurements between two protons dissociated into the opposite directions give information on this process. The measured energies of these protons range from 6 to 14 eV peaked at 9.4 eV[1] (see Fig.1) and found not to change very much over the impact energy of 0.5 - 1 keV. The relative cross sections for double ionization are found to decrease with increasing the impact energy in this energy range, similar to trend in ordinary ionization of atoms and fmolecules. No direct determination of the cross sections of double ionization by electron impact has been reported. From their experimental information, the cross sections are estimated to be of the order of 10^{-20} cm^2 which seems to be in agreement with those in high energy proton impact[2] and in photon impact[3].

References

1) K.E. McCulloh and H.M. Rosenstock, J.Chem. Phys. 48 (1968) 2084.
2) A.E. Edwards, R.M. Wood and R.L. Ezell, Phys. Rev. A 34 (1986) 4411.
3) H.Le Rouzo, J.Phys. B 19 (1986) L677.

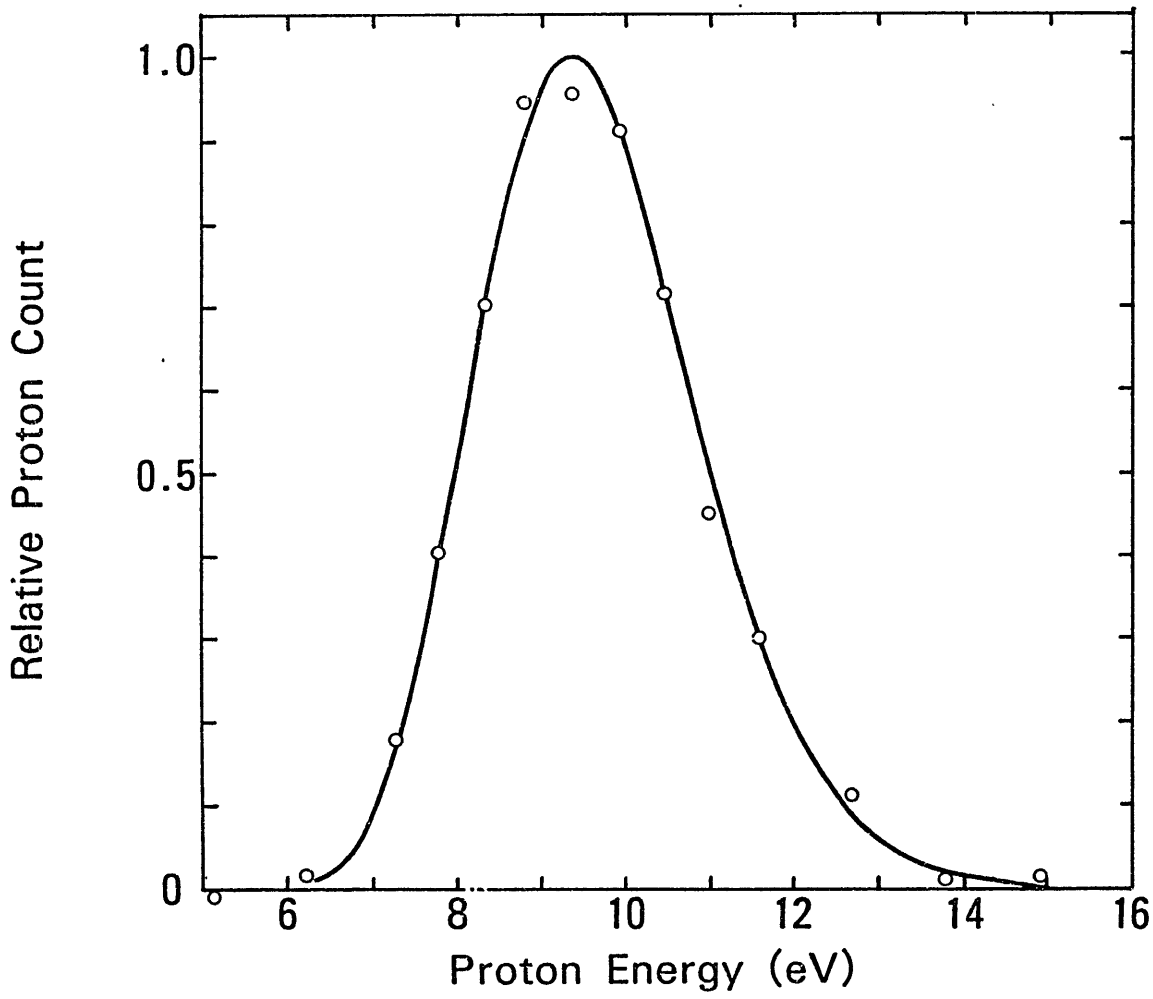

Fig.1 Energy distribution of protons from doubly ionized hydrogen molecules H_2^{2+} in electron impact.

V. Remarks on further AM data

In the edge plasma modelling, more AM data may be necessary. Some of them are described below.

1. The life times of the excited states

Some of the excited molecules have relatively long life times (metastable). They play a role in high density plasma edges where ionization / excitation of such molecules or ions is enhanced. In the followings are described the life times of some states :

$b^3\Sigma_u^+$ state : 10^{-14}s ,	dissociate into H(1s) + H(1s)
$B^1\Sigma_u^+$ state : 10^{-10}s ,	decay into the ground state ($X^1\Sigma_g^+$) via the allowed transition
$a^3\Sigma_g^+$ state : 10^{-8}s ,	decay into $b^3\Sigma_u^+$ state via the allowed transition
$c^3\Pi_u$ (v=0) state : 10^{-3}s,	decay into $b\ ^3\Sigma_u^+$ state via the forbidden magnetic dipole transition
$c^3\Pi_u$ (v≠0) state : 10^{-6}s,	decay into $a^3\Sigma_g^+$ sstate.

Some of these long-lived molecules should have the decay length of the order of meters comparable to the experimental devices in low density plasmas or should have more collisions before decaying. Thus the balance of ionization of plasmas may be affected by the presence of such metastable molecules.

2. The collisions (ionization, excitation, deexcitation) involving species in the excited states

Generally the collision cross sections involving atoms, molecules or their ions in the excited states are expected to be significantly large, compared with those for the ground state species. Such data presently available are very limited. The cross sections for formation and destruction of

such species in the excited states have also to be known. Furthermore, these cross sections involving collisions with surfaces, which are scarce, are requisite for modelling of the edge plasmas.

3. The electron distributions in energy and angle (double differential cross sections)

These double differential cross sections (DDCS) for electrons from H_2 targets have been measured by a number of the investigators. The features for DDCS depend on the particular processes. For example, some have strong dependence on the angle and on the collision energy. The observed features in general agree among experiments. However, the absolute DDCS are sometimes in significant disagreement with each other. In particular, those for low energy electrons differ by one order of the magnitude among different work.

LIST OF IPPJ-AM REPORTS

IPPJ-AM-1* "Cross Sections for Charge Transfer of Hydrogen Beams in Gases and Vapors in the Energy Range 10 eV–10 keV"
H. Tawara (1977) [Published in Atomic Data and Nuclear Data Tables 22, 491 (1978)]

IPPJ-AM-2* "Ionization and Excitation of Ions by Electron Impact –Review of Empirical Formulae–"
T. Kato (1977)

IPPJ-AM-3 "Grotrian Diagrams of Highly Ionized Iron FeVIII-FeXXVI"
K. Mori, M. Otsuka and T. Kato (1977) [Published in Atomic Data and Nuclear Data Tables 23, 196 (1979)]

IPPJ-AM-4 "Atomic Processes in Hot Plasmas and X-Ray Emission"
T. Kato (1978)

IPPJ-AM-5* "Charge Transfer between a Proton and a Heavy Metal Atom"
S. Hiraide, Y. Kigoshi and M. Matsuzawa (1978)

IPPJ-AM-6* "Free-Free Transition in a Plasma –Review of Cross Sections and Spectra–"
T. Kato and H. Narumi (1978)

IPPJ-AM-7* "Bibliography on Electron Collisions with Atomic Positive Ions: 1940 Through 1977"
K. Takayanagi and T. Iwai (1978)

IPPJ-AM-8 "Semi-Empirical Cross Sections and Rate Coefficients for Excitation and Ionization by Electron Collision and Photoionization of Helium"
T. Fujimoto (1978)

IPPJ-AM-9 "Charge Changing Cross Sections for Heavy-Particle Collisions in the Energy Range from 0.1 eV to 10 MeV I. Incidence of He, Li, Be, B and Their Ions"
Kazuhiko Okuno (1978)

IPPJ-AM-10 "Charge Changing Cross Sections for Heavy-Particle Collisions in the Energy Range from 0.1 eV to 10 MeV II. Incidence of C, N, O and Their Ions"
Kazuhiko Okuno (1978)

IPPJ-AM-11 "Charge Changing Cross Sections for Heavy-Particle Collisions in the Energy Range from 0.1 eV to 10 MeV III. Incidence of F, Ne, Na and Their Ions"
Kazuhiko Okuno (1978)

IPPJ-AM-12* "Electron Impact Excitation of Positive Ions Calculated in the Coulomb-Born Approximation –A Data List and Comparative Survey–"
S. Nakazaki and T. Hashino (1979)

IPPJ-AM-13 "Atomic Processes in Fusion Plasmas – Proceedings of the Nagoya Seminar on Atomic Processes in Fusion Plasmas Sept. 5-7, 1979"
Ed. by Y. Itikawa and T. Kato (1979)

IPPJ-AM-14 "Energy Dependence of Sputtering Yields of Monatomic Solids"
N. Matsunami, Y. Yamamura, Y. Itikawa, N. Itoh, Y. Kazumata, S. Miyagawa, K. Morita and R. Shimizu (1980)

IPPJ-AM-15 "Cross Sections for Charge Transfer Collisions Involving Hydrogen Atoms"
Y. Kaneko, T. Arikawa, Y. Itikawa, T. Iwai, T. Kato, M. Matsuzawa, Y. Nakai, K. Okubo, H. Ryufuku, H. Tawara and T. Watanabe (1980)

IPPJ-AM-16 "Two-Centre Coulomb Phaseshifts and Radial Functions"
H. Nakamura and H. Takagi (1980)

IPPJ-AM-17 "Empirical Formulas for Ionization Cross Section of Atomic Ions for Electron Collisions –Critical Review with Compilation of Experimental Data–"
Y. Itikawa and T. Kato (1981)

IPPJ-AM-18 "Data on the Backscattering Coefficients of Light Ions from Solids"
T. Tabata, R. Ito, Y. Itikawa, N. Itoh and K. Morita (1981) [Published in Atomic Data and Nuclear Data Tables 28, 493 (1983)]

IPPJ-AM-19 "Recommended Values of Transport Cross Sections for Elastic Collision and Total Collision Cross Section for Electrons in Atomic and Molecular Gases"
M. Hayashi (1981)

IPPJ-AM-20 "Electron Capture and Loss Cross Sections for Collisions between Heavy Ions and Hydrogen Molecules"
Y. Kaneko, Y. Itikawa, T. Iwai, T. Kato, Y. Nakai, K. Okuno and H. Tawara (1981)

IPPJ-AM-21 "Surface Data for Fusion Devices – Proceedings of the U.S–Japan Workshop on Surface Data Review Dec. 14-18, 1981"
Ed. by N. Itoh and E.W. Thomas (1982)

IPPJ-AM-22 "Desorption and Related Phenomena Relevant to Fusion Devices"
Ed. by A. Koma (1982)

IPPJ-AM-23 "Dielectronic Recombination of Hydrogenic Ions"
T. Fujimoto, T. Kato and Y. Nakamura (1982)

IPPJ-AM-24 "Bibliography on Electron Collisions with Atomic Positive Ions: 1978 Through 1982 (Supplement to IPPJ-AM-7)"
Y. Itikawa (1982) [Published in Atomic Data and Nuclear Data Tables 31, 215 (1984)]

IPPJ-AM-25 "Bibliography on Ionization and Charge Transfer Processes in Ion-Ion Collision"
H. Tawara (1983)

IPPJ-AM-26 "Angular Dependence of Sputtering Yields of Monatomic Solids"
Y. Yamamura, Y. Itikawa and N. Itoh (1983)

IPPJ-AM-27 "Recommended Data on Excitation of Carbon and Oxygen Ions by Electron Collisions"
Y. Itikawa, S. Hara, T. Kato, S. Nakazaki, M.S. Pindzola and D.H. Crandall (1983) [Published in Atomic Data and Nuclear Data Tables 33, 149 (1985)]

IPPJ-AM-28 "Electron Capture and Loss Cross Sections for Collisions Between Heavy Ions and Hydrogen Molecules (Up-dated version of IPPJ-AM-20)
H. Tawara, T. Kato and Y. Nakai (1983) [Published in Atomic Data and Nuclear Data Tables 32, 235 (1985)]

IPPJ-AM-29 "Bibliography on Atomic Processes in Hot Dense Plasmas"
T. Kato, J. Hama, T. Kagawa, S. Karashima, N. Miyanaga, H. Tawara, N. Yamaguchi, K. Yamamoto and K. Yonei (1983)

IPPJ-AM-30 "Cross Sections for Charge Transfers of Highly Ionized Ions in Hydrogen Atoms (Up-dated version of IPPJ-AM-15)"
H. Tawara, T. Kato and Y. Nakai (1983) [Published in Atomic Data and Nuclear Data Tables 32, 235 (1985)]

IPPJ-AM-31 "Atomic Processes in Hot Dense Plasmas"
T. Kagawa, T. Kato, T. Watanabe and S. Karashima (1983)

IPPJ-AM-32 "Energy Dependence of the Yields of Ion-Induced Sputtering of Monatomic Solids"
N. Matsunami, Y. Yamamura, Y. Itikawa, N. Itoh, Y. Kazumata, S. Miyagawa, K. Morita, R. Shimizu and H. Tawara (1983) [Published in Atomic Data and Nuclear Data Tables 31, 1 (1984)]

IPPJ-AM-33 "Proceedings on Symposium on Atomic Collision Data for Diagnostics and Modelling of Fusion Plasmas, Aug. 29 – 30, 1983"
Ed. by H. Tawara (1983)

IPPJ-AM-34 "Dependence of the Backscattering Coefficients of Light Ions upon Angle of Incidence"
T. Tabata, R. Ito, Y. Itikawa, N. Itoh, K. Morita and H. Tawara (1984)

IPPJ-AM-35 "Proceedings of Workshop on Synergistic Effects in Surface Phenomena Related to Plasma-Wall Interactions, May 21 – 23, 1984"
Ed. by N. Itoh, K. Kamada and H. Tawara (1984) [Published in Radiation Effects 89, 1 (1985)]

IPPJ-AM-36 "Equilibrium Charge State Distributions of Ions ($Z_1 \geqq 4$) after Passage through Foils – Compilation of Data after 1972"
K. Shima, T. Mikumo and H. Tawara (1985) [Published in Atomic Data and Nuclear Data Tables 34, 357 (1986)]

IPPJ-AM-37 "Ionization Cross Sections of Atoms and Ions by Electron Impact"
H. Tawara, T. Kato and M. Ohnishi (1985) [Published in Atomic Data and Nuclear Data Tables 36, 167 (1987)]

IPPJ-AM-38 "Rate Coefficients for the Electron-Impact Excitations of C-like Ions"
Y. Itikawa (1985)

IPPJ-AM-39 "Proceedings of the Japan-U.S. Workshop on Impurity and Particle Control, Theory and Modeling, Mar. 12 – 16, 1984"
Ed. by T. Kawamura (1985)

IPPJ-AM-40 "Low-Energy Sputterings with the Monte Carlo Program ACAT"
Y. Yamamura and Y. Mizuno (1985)

IPPJ-AM-41 "Data on the Backscattering Coefficients of Light Ions from Solids (a Revision)"
R. Ito, T. Tabata, N. Itoh, K. Morita, T. Kato and H. Tawara (1985)

IPPJ-AM-42 "Stopping Power Theories for Charged Particles in Inertial Confinement Fusion Plasmas (Emphasis on Hot and Dense Matters)"
S. Karashima, T. Watanabe, T. Kato and H. Tawara (1985)

IPPJ-AM-43 "The Collected Papers of Nice Project/IPP, Nagoya"
Ed. by H. Tawara (1985)

IPPJ-AM-44 "Tokamak Plasma Modelling and Atomic Processes"
Ed. by T. Kawamura (1986)

IPPJ-AM-45 Bibliography of Electron Transfer in Ion-Atom Collisions
H. Tawara, N. Shimakura, N. Toshima and T. Watanabe (1986)

IPPJ-AM-46 "Atomic Data Involving Hydrogens Relevant to Edge Plasmas"
H. Tawara, Y. Itikawa, Y. Itoh, T. Kato, H. Nishimura, S. Ohtani, H. Takagi, K. Takayanagi and M. Yoshino (1986)

IPPJ-AM-47 "Resonance Effects in Electron-Ion Collisions"
Ed. by H. Tawara and G. H. Dunn (1986)

IPPJ-AM-48 "Dynamic Processes of Highly Charged Ions (Proceedings)"
Ed. by Y. Kanai and S. Ohtani (1986)

IPPJ-AM-49 "Wavelengths of K X-Rays of Iron Ions"
T. Kato, S. Morita and H. Tawara (1987)

IPPJ-AM-50 "Proceedings of the Japan-U.S. Workshop P-92 on Plasma Material Interaction/High Heat Flux Data Needs for the Next Step Ignition and Steady State Devices, Jan. 26 – 30, 1987"
Ed. by A. Miyahara and K. L. Wilson (1987)

IPPJ-AM-51 "High Heat Flux Experiments on C-C Composite Materials by Hydrogen Beam at the 10MW Neutral Beam Injection Test Stand of the IPP Nagoya"
H. Bolt, A. Miyahara, T. Kuroda, O. Kaneko, Y. Kubota, Y. Oka and K. Sakurai (1987)

IPPJ-AM-52 "Energy Dependence of Ion-Induced Sputtering Yields of Monatomic Solids in the Low Energy Region"
N. Matsunami, Y. Yamamura, N. Itoh, H. Tawara and T. Kawamura (1987)

IPPJ-AM-53 "Data Base on the High Heat Flux Behaviour of Metals and Carbon Materials for Plasma Facing Components – Experiments at the 10 MW Neutral Beam Injection Test Stand of the IPP Nagoya"
H. Bolt, C. D. Croessmann, A. Miyahara, T. Kuroda and Y. Oka (1987)

IPPJ-AM-54 "Final (n, ℓ) State-Resolved Electron Capture by Multiply Charged Ions from Neutral Atoms"
N. Shimakura, N. Toshima, T. Watanabe and H. Tawara (1987)

IPPJ-AM-55 "Atomic Data for Hydrogens in Collisions with Electrons – Addenda to IPPJ-AM-46"
H. Tawara, Y. Itikawa, H. Nishimura and M. Yoshino (1987)

Available upon request to Research Information Center, Institute of Plasma Physics, Nagoya University, Nagoya 464, Japan, except for the reports noted with*.

Corrections to IPPJ-AM-46 (1986)

Please replace Figs.1, 2 and 32 with new figures enclosed here.

and make the following corrections :

	incorrect	correct
p.6, ℓ.3	; $2e + H^+ + H \rightarrow$	$2e + H^+ + H$ / $3e + H^+ + H^+$
p.8, ℓ.3	; $H_3 + H_2 \rightarrow$	$H_3^+ + H_2$
p.18, ℓ.12-13	; Figs.5-7 and 9-13 →	Figs.5-11 and 13
p.40, ℓ.6	; eq.(3) →	$H^+ + H^+ + 3e$
p.51, ℓ.14	; remove "significant".	
p.76, ℓ.22	; photon energy from threshold →	photon energy up
p.76, ℓ.26	; 2pπu →	$2p\pi_u$
p.77, ℓ.1	; 6.89 →	6.9
p.77, ℓ.2	; add at the end.	at 300 K
p.80	; caption in the figure	
	$H_2^+(K) + h\nu \rightarrow$	$H_2^+[T(K)] + h\nu$
p.133	; unit in the ordinate	
	$cm^3 \rightarrow$	cm^6

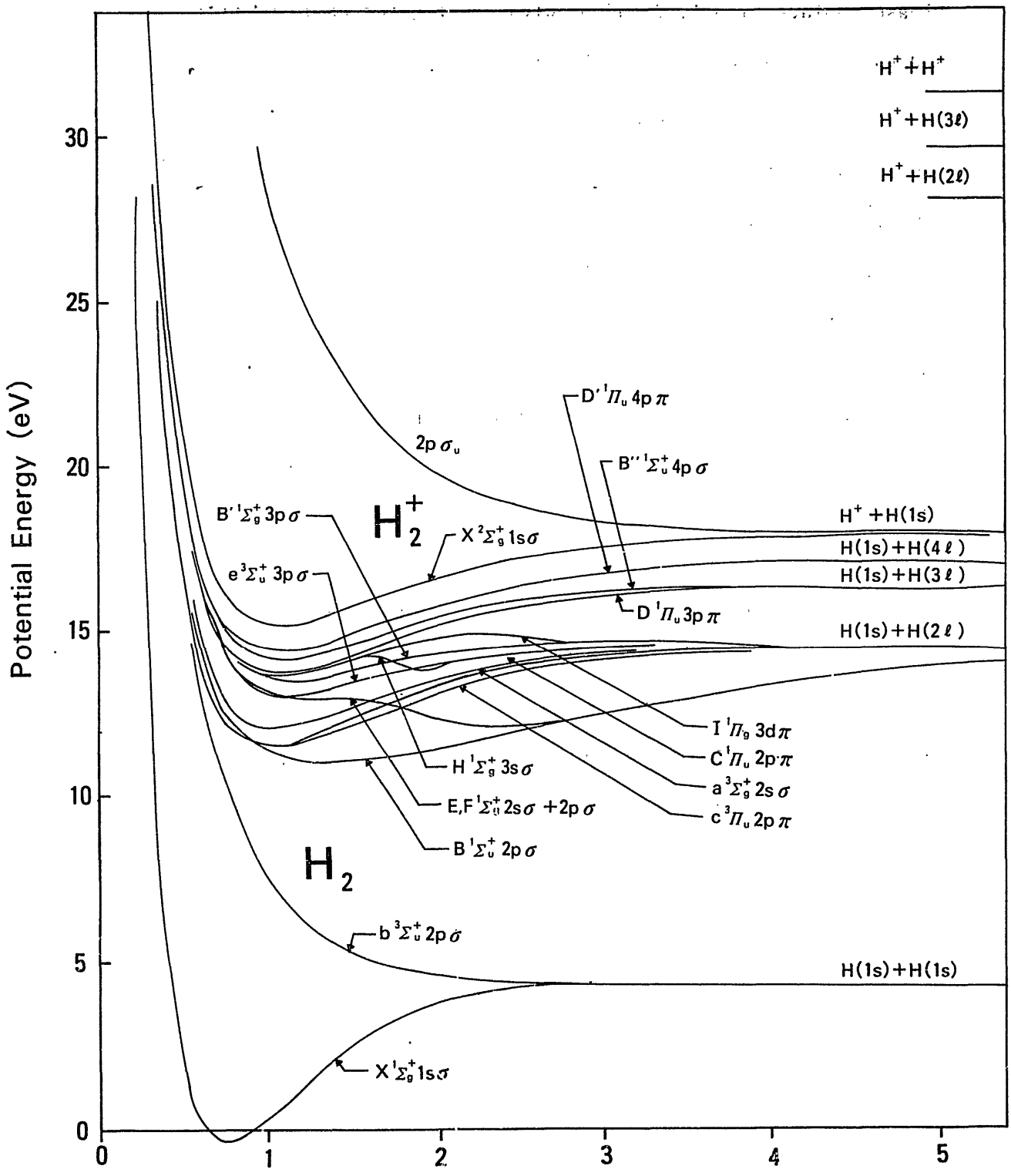
Potential Energy (eV)
Internuclear Distance (Å)
H⁺+H⁺
H⁺+H(3ℓ)
H⁺+H(2ℓ)
H⁺+H(1s)
H(1s)+H(4ℓ)
H(1s)+H(3ℓ)
H(1s)+H(2ℓ)
H(1s)+H(1s)
H₂⁺
H₂
2pσu
D' ¹Πu 4pπ
B'' ¹Σu⁺ 4pσ
B' ¹Σg⁺ 3pσ
X ²Σg⁺ 1sσ
e ³Σu⁺ 3pσ
D ¹Πu 3pπ
I ¹Πg 3dπ
C ¹Πu 2pπ
a ³Σg⁺ 2sσ
c ³Πu 2pπ
H ¹Σg⁺ 3sσ
E,F ¹Σg⁺ 2sσ +2pσ
B ¹Σu⁺ 2pσ
b ³Σu⁺ 2pσ
X ¹Σg⁺ 1sσ
0
5
10
15
20
25
30
0
1
2
3
4
5

Fig. 1

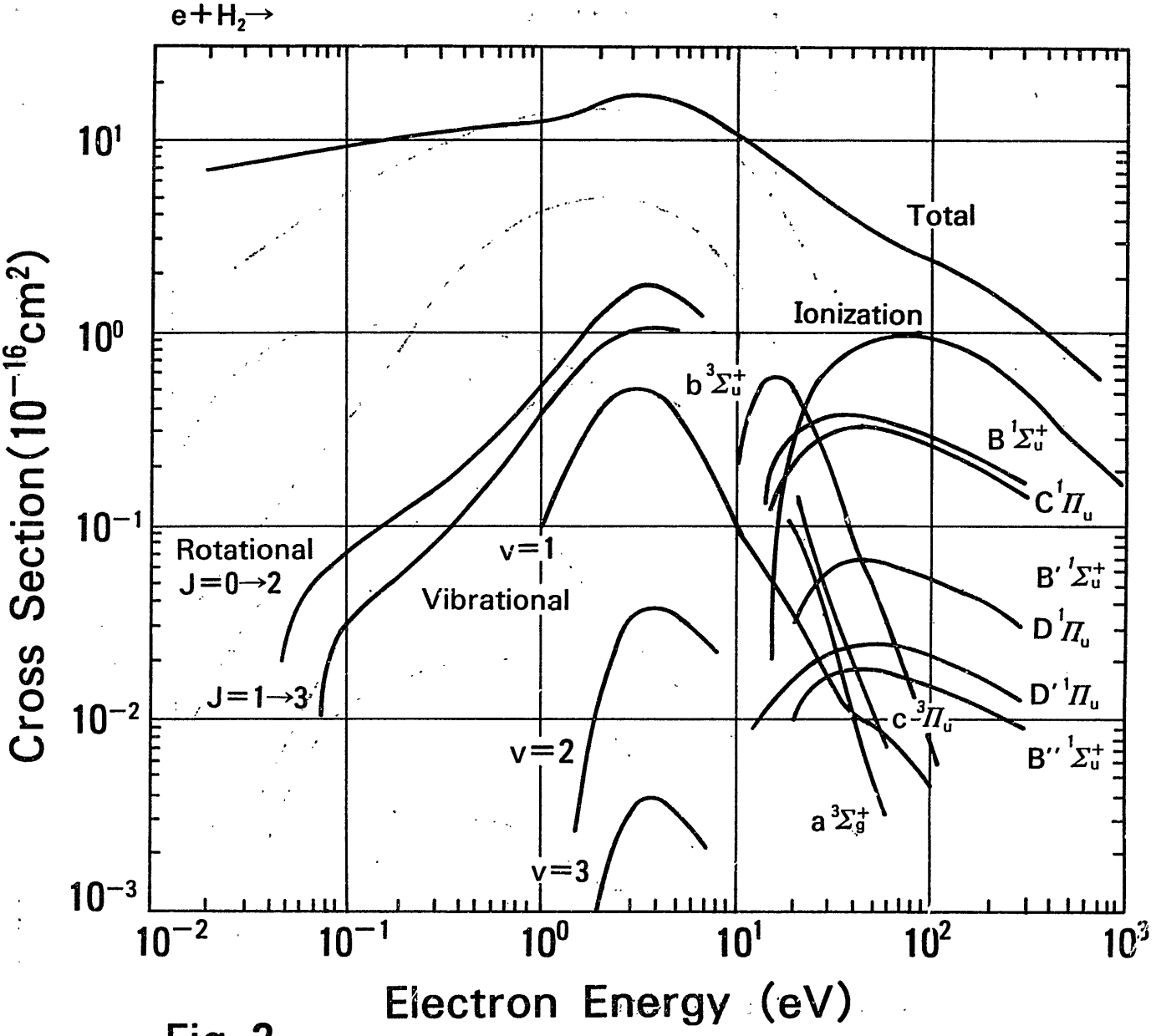
e+H2→
Cross Section(10−16cm2)
Electron Energy (eV)
Total
Ionization
b 3Σu+
B 1Σu+
C 1Πu
B' 1Σu+
D 1Πu
D' 1Πu
c 3Πu
B'' 1Σu+
a 3Σg+
Rotational
J=0→2
J=1→3
Vibrational
v=1
v=2
v=3

Fig. 2

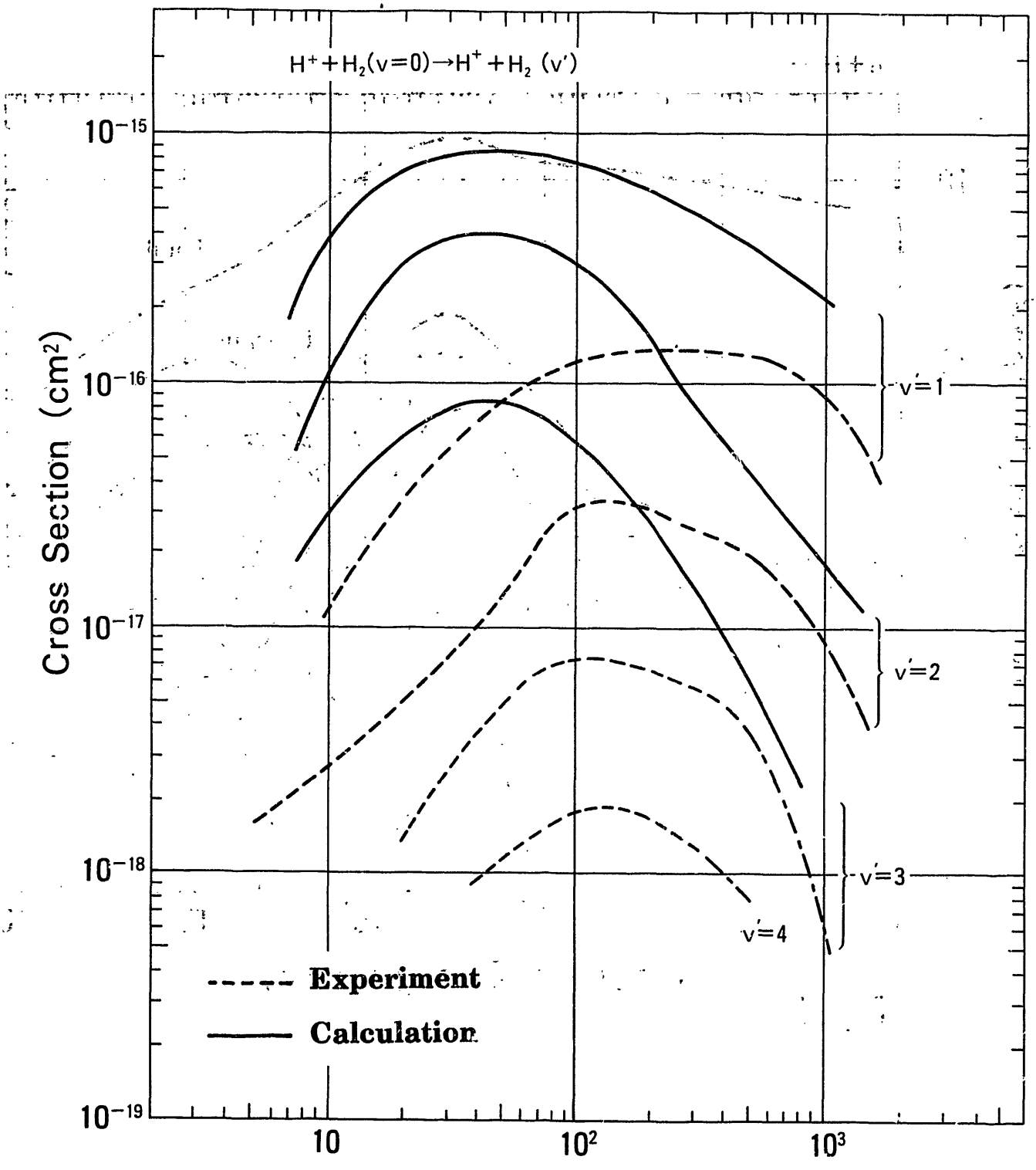
H⁺+H₂(v=0)→H⁺+H₂ (v')
Cross Section (cm²)
10⁻¹⁵
10⁻¹⁶
10⁻¹⁷
10⁻¹⁸
10⁻¹⁹
10
10²
10³
Collision Energy (eV/amu)
v'=1
v'=2
v'=3
v'=4
Experiment
Calculation

Fig. 32